

1 **A genomic assessment of the marine-speciation paradox within the toothed whale**
2 **superfamily Delphinoidea**

3
4
5 Michael V Westbury^{1*}, Andrea A. Cabrera¹, Alba Rey-Iglesia¹, Binia De Cahsan¹, David A.
6 Duchêne¹, Stefanie Hartmann², Eline D Lorenzen^{1*}

- 7 1. GLOBE Institute, University of Copenhagen, Øster Voldgade 5-7, Copenhagen,
8 Denmark
9 2. Institute of Biochemistry and Biology, University of Potsdam, Karl-Liebknecht-Str.
10 24-25, Potsdam, Germany

11 * Corresponding authors: m.westbury@sund.ku.dk, elinelorenzen@sund.ku.dk

12
13 **Abstract**

14
15 Understanding speciation is a central endeavour in Biology. The formation of new
16 species was once thought to be a simple bifurcation process. However, recent advances in
17 genomic resources now provide the opportunity to investigate the role of post-divergence
18 gene flow in the speciation process. The diversification of lineages in the presence of gene
19 flow appears paradoxical. However, with enough time and in the presence of incomplete
20 physical and/or ecological barriers to gene flow, speciation can and does occur. Speciation
21 without complete isolation appears especially likely to occur in highly mobile, wide-ranging
22 marine species, such as cetaceans, which face limited geographic barriers. The toothed whale
23 superfamily Delphinoidea represents a good example to further explore speciation in the
24 presence of interspecific gene flow. Delphinoidea consists of three families (Delphinidae,
25 Phocoenidae, Monodontidae) and within all three families, contemporary interspecific
26 hybrids have been reported. Here, we utilise publicly available genomes from nine species,
27 representing all three Delphinoidea families, to investigate signs of post-divergence gene
28 flow across their genomes, and to shed light on the speciation processes that led to the current
29 diversity of the superfamily. We use a multifaceted approach including: (i) phylogenetics, (ii)
30 the distribution of shared derived alleles, and (iii) demographic inference. We find that the
31 divergence and evolution of lineages in Delphinoidea did not follow a process of pure
32 bifurcation, but were much more complex. Our results indicate multiple ancestral gene flow
33 events within and among families, which may have occurred millions of years after initial
34 divergence.

35
36 **Introduction**

37
38 The formation of new species involves the divergence of lineages through
39 reproductive isolation. Such isolation can initially occur in allopatry (geographical isolation)
40 or in sympatry (biological/ecological isolation). Over time, these barriers are maintained and
41 strengthened, ultimately leading to the formation of new species (Norris and Hull, 2012).
42 While allopatric speciation requires geographical isolation plus time, sympatric speciation

43 often requires a broader and more complicated set of mechanisms (Turelli et al., 2001). These
44 mechanisms mostly rely on ecologically-mediated natural selection. Parapatric speciation, on
45 the other hand, encompasses intermediate scenarios of partial, but incomplete, physical
46 restrictions to gene flow leading to speciation.

47

48 Through the analysis of whole-genome datasets, the detection of post-divergence gene
49 flow between distinct species is becoming commonplace (Árnason et al., 2018; Barlow et al.,
50 2018; Westbury et al., 2020), demonstrating that speciation is much more complex than a
51 simple bifurcating process (Campbell and Poelstra, 2018; Feder et al., 2012). Speciation is
52 not an instantaneous process, but requires tens of thousands to millions of generations to
53 achieve complete reproductive isolation (Butlin and Smadja, 2018; Coyne and Orr, 2004; Liu
54 et al., 2014). The duration it takes to reach this isolation may be especially long in highly
55 mobile marine species, such as cetaceans, due to a relative lack of geographic barriers in the
56 marine realm, and therefore high potential for secondary contact and gene flow (Árnason et
57 al., 2018).

58

59 The apparent inability to undergo allopatric speciation in marine species has been
60 termed the marine-speciation paradox (Bierne et al., 2003). However, over the past decade,
61 genomic studies have provided some insights into how speciation can occur within cetaceans
62 (Árnason et al., 2018; Moura et al., 2020). For example, initial phases of allopatry among
63 populations of killer whales (*Orcinus orca*) may have led to the accumulation of ecological
64 differences between populations, which strengthened population differences even after
65 secondary contact (Foote et al., 2011; Foote and Morin, 2015). However, whether these initial
66 phases of allopatry caused the divergence, or whether speciation occurred purely in sympatry,
67 remains debated (Moura et al., 2015). But, these two hypotheses are not necessarily mutually
68 exclusive. Instead, differentiation in parapatry, encompassing features of both allopatric and
69 sympatric speciation, may have been key in the evolutionary history of cetaceans.

70

71 The toothed whale superfamily Delphinoidea represents an interesting opportunity to
72 further explore speciation in the presence of putative interspecific gene flow. The crown root
73 of Delphinoidea has been dated at ~19 million years ago (Ma) (95% CI 19.73 - 18.26 Ma)
74 (McGowen et al., 2020) and has given rise to three families: (i) Delphinidae, the most
75 species-rich family, which comprises dolphins and ‘black-fish’ (such as killer whales and
76 pilot whales (*Globicephala spp.*)); (ii) Phocoenidae, commonly known as porpoises; and (iii)
77 Monodontidae, which comprises two surviving lineages, beluga (*Delphinapterus leucas*) and
78 narwhal (*Monodon monoceros*).

79

80 Delphinoidea is of particular interest, as contemporary interspecific hybrids have been
81 reported within all three families (Delphinidae: (Espada et al., 2019; Miyazaki et al., 1992;
82 Silva et al., 2005); Phocoenidae: (Willis et al., 2004); Monodontidae: (Skovrind et al., 2019).
83 However, these hybrids represent recent hybridization events that occurred long after species
84 divergence, and their contribution to the parental gene pools is mostly unknown. The
85 presence of more ancient introgressive hybridization events between families, and during the
86 early radiations of these families, has yet to be investigated. With the rapid increase of

87 genomic resources for cetaceans, and in particular for species within Delphinoidea, we are
88 presented with the ideal opportunity to investigate post-divergence gene flow between
89 lineages, furthering our understanding of speciation processes in cetaceans.

90

91 Here, we utilise publicly available whole-genome data from nine species of
92 Delphinoidea, representing all three families, to investigate signs of post-divergence gene
93 flow across their genomes. Our analyses included five Delphinidae (killer whale, Pacific
94 white-sided dolphin (*Lagenorhynchus obliquidens*), long-finned pilot whale (*Globicephala*
95 *melas*), bottlenose dolphin (*Tursiops truncatus*), Indo-Pacific bottlenose dolphin (*T.*
96 *aduncus*)); two Phocoenidae (harbour porpoise (*Phocoena phocoena*), finless porpoise
97 (*Neophocaena phocaenoides*)); and two Monodontidae (beluga, narwhal). Moreover, we
98 compare their species-specific genetic diversity and demographic histories, and explore how
99 species abundances may have played a role in interspecific hybridisation over the last two
100 million years.

101

102 **Results and discussion**

103

104 **Detecting gene flow**

105 To assess the evolutionary relationships across the genomes of the nine Delphinoidea
106 species investigated, we computed non-overlapping sliding-window maximum-likelihood
107 phylogenies of four different window sizes in RAxML (Stamatakis, 2014). These analyses
108 resulted in 43,207 trees (50 kilobase (kb) windows), 21,387 trees (100 kb windows), 3,705
109 trees (500 kb windows), and 1,541 trees (1 megabase (Mb) windows) (Fig. 1, Supplementary
110 Fig. S1, Supplementary Table S1). The 50 kb windows retrieved a total of 96 unique
111 topologies, 100 kb windows retrieved 47 unique topologies, 500 kb windows retrieved 16
112 unique topologies, and 1 Mb windows retrieved 15 unique topologies. Regardless of window
113 size, we retrieve consensus support for the species tree previously reported using target-
114 sequence capture (McGowen et al., 2020). However, when considering the smallest window
115 size (50 kb), we find a considerable proportion of trees (up to 76%) with an alternative
116 topology to the known species tree (Fig. 1A). These alternative topologies may be due to
117 incomplete lineage sorting (ILS) or to interspecific gene flow (Leaché et al., 2014).
118 Moreover, the higher prevalence of this pattern in the 50 kb windows (for example, 21% of
119 windows show an alternative topology in the 1 Mb dataset (Fig. 1B)), may indicate that
120 inconsistencies in topology are caused by ancient, rather than recent, events.

121

122 We explored whether the large number of phylogenetic discrepancies in the 50kb
123 windows could be linked to the GC content (%GC) of the windows. Discrepancies could
124 arise, as elevated levels of GC content can result from higher levels of GC-Biased Gene
125 Conversion (gBGC) in regions with higher levels of recombination (Lartillot, 2013). When
126 binning windows into either high, medium, or low levels of GC content, the most common
127 topologies are consistent, but with slight differences in overall values (Supplementary Table
128 S2). This result suggests that the topological discrepancies are not arising purely due to GC-
129 content linked biases and recombination rate.

130

131 To investigate whether the alternative topologies could simply be explained by ILS,
132 or whether a combination of ILS and gene flow was a more probable cause, we ran
133 Quantifying Introgression via Branch Lengths (QuIBL) (Edelman et al., 2019) on every
134 twentieth tree from the 50 kb sliding-window analysis (Supplementary Table S3), as well as
135 on a dataset that contained trees constructed using 20 kb windows with a 1 Mb slide
136 (Supplementary Table S4). As we did not recover any large numbers of phylogenetic
137 discrepancies between families, we were only able to look at the potential cause of
138 discrepancies in the Delphinidae family. Our QuIBL analyses suggest that the different
139 retrieved topologies cannot be explained by ILS alone, but a combination of both ILS and
140 gene flow.

141

142 To further explore potential gene flow while taking ILS into account, we applied D-
143 statistics. D-statistics use a four-taxon approach [[H1, H2], H3], Outgroup] to uncover the
144 differential distribution of shared derived alleles, which may represent gene flow between
145 either H1/H3 or H2/H3. Here we used baiji (*Lipotes vexillifer*) as the outgroup, and alternated
146 ingroup positions based on the consensus topology. We find that 85 out of 86 tests show
147 signs of gene flow within and between families (Supplementary Table S5), suggesting the
148 evolutionary history of Delphinoidea was more complex than a simple bifurcating process.

149

150 Due to the inability of the four-taxon D-statistics approach to detect the direction of
151 gene flow, as well as whether gene flow events may have occurred between ancestral
152 lineages, we used D-foil. D-foil enables further characterization of the D-statistics results,
153 which may be particularly relevant given the complex array of gene flow putatively present
154 within Delphinoidea. D-foil uses a five-taxon approach [[H1, H2] [H3, H4], Outgroup] and a
155 system of four independent D-statistics in a sliding-window fashion to uncover (i) putative
156 gene flow events, (ii) donor and recipient lineages, and (iii) whether gene flow events
157 occurred between a distantly related lineage and the ancestor of two sister lineages, which is
158 indicative of ancestral-lineage gene flow. However, due to the input topology requirements of
159 D-foil, we were only able to investigate gene flow between families, and not within families,
160 using this analysis. Hence, we tested for gene flow between Delphinidae/Phocoenidae,
161 Delphinidae/Monodontidae, and Monodontidae/Phocoenidae.

162

163 The D-foil results underscore the complex pattern of post-divergence gene flow
164 between families indicated by the D-statistics. We find support for interfamilial gene flow
165 events between all nine species investigated, to varying extents (Supplementary Table S6).
166 This could reflect multiple episodes of gene flow between all investigated species.
167 Alternatively, the pattern could reflect ancient gene flow events between the ancestors of H1-
168 H2 and H3-H4 (in the topology [[H1, H2] [H3, H4], Outgroup]), with differential inheritance
169 of the admixed loci in subsequent lineages. Such ancestral gene flow events have previously
170 been shown to lead to false positives between species pairs using D-statistics (Moodley et al.,
171 2020). A further putative problem with these results can be seen when implementing D-foil
172 on the topology [[Delphinidae, Delphinidae], [Monodontidae, Phocoenidae], Outgroup]. We
173 find the majority of windows support a closer relationship between Delphinidae (ancestors of
174 H1 and H2) and Monodontidae (H3), as opposed to the species tree. If this result is correct, it

175 suggests the input topology was incorrect, implying that Delphinidae and Monodontidae are
176 sister lineages, as opposed to Phocoenidae and Monodontidae. However, this contrasts with
177 the family topology of [Delphinidae, [Phocoenidae, Monodontidae]] retrieved in our
178 phylogenetic analyses (Fig. 1) and reported by others (McGowen et al., 2020; Steeman et al.,
179 2009). Instead, we suggest our result reflects the limited ability of D-foil to infer gene flow
180 between these highly divergent lineages.

181

182 False positives and potential biases in D-statistics and D-foil can arise due to a
183 number of factors including (i) ancestral population structure, (ii) introgression from
184 unsampled and/or extinct ghost lineages, (iii) differences in relative population size of
185 lineages or in the timing of gene flow events, (iv) different evolutionary rates or sequencing
186 errors between H1 and H2, and (v) gene flow between ancestral lineages (Moodley et al.,
187 2020; Slatkin and Pollack, 2008; Zheng and Janke, 2018). These issues are important to
188 consider when interpreting our results, as the deep divergences of lineages suggest there were
189 probably a number of ancestral gene flow events, as well as gene flow events between now-
190 extinct lineages, that may bias results.

191

192 **Cessation of lineage sorting and/or gene flow**

193 To further elucidate the complexity of interspecific gene flow within Delphinoidea,
194 we implemented F1 hybrid PSMC (hPSMC) (Cahill et al., 2016). This method creates a
195 pseudo-diploid sequence by merging pseudo-haploid sequences from two different genomes,
196 which in our case represents two different species. The variation in the interspecific pseudo-
197 F1 hybrid genome cannot coalesce more recently than the emergence of reproductive
198 isolation between the two parental species. If some regions within the genomes of two target
199 species are yet to fully diverge, due to ILS or to gene flow, hybridisation may still be
200 possible. Therefore, we use this method to infer when reproductive isolation between two
201 species may have occurred.

202

203 When considering the uppermost limit of when two target genomes coalesce
204 (equating the oldest date), and the lower confidence interval of each divergence date
205 (equating the most recent date) (McGowen et al., 2020), we find the majority of comparisons
206 (29/36) show lineage sorting and/or gene flow occurred for >50% of the post-divergence
207 branch length (Fig. 2, Supplementary results). However, as we used divergence dates
208 estimated assuming a fixed tree-like topology without ILS or gene flow (McGowen et al.,
209 2020), the divergence dates we use may be overestimated. Nevertheless, our results suggest
210 that reaching complete reproductive isolation in Delphinoidea was a slow process, due to ILS
211 and/or gene flow. ILS levels are known to be proportional to ancestral population sizes, and
212 inversely proportional to time between speciation events (Pamilo and Nei, 1988). Hence, if
213 ILS was the only explanation for this phenomenon, this would suggest extremely large
214 ancestral population sizes. An alternative explanation is the occurrence of gene flow after
215 initial divergence, supported by our phylogenetic and D-statistics results above. Post-
216 divergence gene flow may reflect the ability of cetacean species to travel long distances, and
217 the absence of significant geographical barriers in the marine environment. Alternatively, if

218 geographic barriers did drive initial divergence, the pattern retrieved in our data may reflect
219 secondary contact prior to complete reproductive isolation.

220

221 Despite our finding of long-term gene flow in the majority of species comparisons,
222 our results suggest that lineage sorting is complete and that gene flow has ceased between all
223 lineages in our dataset. This finding is in contrast with confirmed reports of fertile
224 contemporary hybrids between several of our target species, and may reflect the inability of
225 hPSMC to detect low levels of migration. For example, viable offspring have been reported
226 between bottlenose dolphins and both Indo-Pacific bottlenose dolphins (Gridley et al., 2018)
227 and Pacific white-sided dolphins (Crossman et al., 2016; Miyazaki et al., 1992). Simulations
228 have shown that in the presence of as few as 1/10,000 migrants per generation, hPSMC will
229 suggest continued gene flow. However, this is not the case with a rate $< 1/100,000$ migrants
230 per generation. Rather, in the latter case, the exponential increase in N_e of the pseudo-hybrid
231 genome, which can be used to infer the date at which gene flow ceased between the parental
232 species, becomes a more gradual transition, leading to a larger estimated time interval of gene
233 flow (Cahill et al., 2016). Within Delphinidae, we observe a less pronounced increase in N_e
234 in the pseudo-hybrids, suggesting continued, but very low migration rates (Supplementary
235 results). This finding suggests that gene flow within Delphinidae may have continued for
236 longer than shown by hPSMC, which may not be sensitive enough to detect low rates of
237 recent gene flow. Either way, our hPSMC results within and between all three families show
238 a consistent pattern of long periods of lineage sorting/gene flow in Delphinoidea, some
239 lasting up to more than ten million years post divergence.

240

241 We further assessed the robustness of our hPSMC results to the inclusion or exclusion
242 of repeat regions in the pseudodiploid genome. We compared the hPSMC results when
243 including and removing repeat regions for three independent species pairs of varying levels
244 of phylogenetic distance. These included a shallow divergence (bottlenose and Indo-Pacific
245 bottlenose dolphins), medium divergence (beluga and narwhal), and deep divergence
246 (bottlenose dolphin and beluga) (Supplementary Figs. S2 - S4). For all species pairs, results
247 showed that pre-divergence N_e is almost identical, and the exponential increase in N_e is just
248 slightly more recent when removing the repeat regions, compared to when repeat regions are
249 included. This gives us confidence that the inclusion of repeats did not greatly influence our
250 results.

251

252 To add independent evidence for continued lineage sorting/gene flow for an extended
253 period after initial divergence, we compared relative divergence time between killer whale,
254 Pacific white-sided dolphin, and long-finned pilot whale based on the species tree and a set of
255 alternative topologies (Supplementary figure S5). We focused on Delphinidae due to the
256 large number of loci per alternative topology (Supplementary Tables S1, S2, S3, and S4). By
257 assuming ILS and gene flow are the dominant forces behind gene-tree discordance, we can
258 uncover information about the timing of ILS and gene flow events among lineages, by
259 isolating the loci that produce each topology (Mendes and Hahn, 2016). In agreement with
260 our hPSMC results, this analysis shows that ILS/gene flow continued for a long time after
261 initial divergence. For example, we observe that the killer whale diverges from all other

262 Delphinidae at a relative divergence time of 0.45 (45% of the divergence time of
263 Delphinoidea and the baiji) in the consensus topology (Supplementary figure S5A). In an
264 alternative topology, the killer whale is placed as sister to the Pacific white-sided dolphin
265 (Supplementary figure S5B); despite still diverging from the remaining Delphinidae at
266 approximately the same relative timing (0.42), it diverges from the Pacific white-sided
267 dolphin at a relative divergence time of 0.25. As we assume the alternative topologies only
268 arise due to ILS and/or gene flow, this suggests lineage sorting and/or gene flow continued
269 along ~40% of the post-divergence branch length. This estimate is qualitatively equivalent to
270 that made using hPSMC (minimally 43%). Similarly, long periods of post-divergence lineage
271 sorting/gene flow are observed when investigating topologies with the killer whale and long-
272 finned pilot whale as sister species (Supplementary figure S5C, ~43%), and with the Pacific
273 white-sided dolphin and long-finned pilot whale as sister species (Supplementary figure S5D,
274 ~37%).

275

276 The alternative topologies may have arisen due to ILS alone. However, for ILS to
277 have continued for so long after initial divergence would suggest very large effective
278 population sizes in all lineages involved. In summary, by combining findings from several
279 analyses, and with the knowledge that interspecific hybridisation is still ongoing between
280 many of the lineages studied here, we suggest that both ILS and gene flow played a major
281 role in the speciation of Delphinoidea.

282

283 **Interspecific hybridisation**

284

285 Making inferences as to what biological factors lead to interspecific hybridisation is
286 challenging, as many variables may play a role. One hypothesis is that interspecific
287 hybridization may occur at a higher rate during periods of low abundance, when a given
288 species encounters only a limited number of conspecifics (Crossman et al., 2016; Edwards et
289 al., 2011; Westbury et al., 2019). When considering species that have not yet undergone
290 sufficient divergence, preventing their ability to hybridise, individuals may mate with a
291 closely-related species, instead of investing energy in finding a relatively rarer conspecific
292 mate.

293

294 To explore the relationship between susceptibility to interspecific hybridisation and
295 population size, we calculated the level of genome-wide genetic diversity for each species, as
296 a proxy for their population size (Fig. 3A). Narwhal, killer whale, beluga, and long-finned
297 pilot whale have the lowest diversity levels, respectively, and should therefore be more
298 susceptible to interspecific hybridization events. A beluga/narwhal hybrid has been reported
299 (Skovrind et al., 2019), as has hybridisation between long-finned and short-finned pilot
300 whales (Miralles et al., 2016). However, hybrids between species with high genetic diversity,
301 including harbour porpoise (Willis et al., 2004), Indo-Pacific bottlenose dolphin (Baird et al.,
302 2012), and bottlenose dolphin (Espada et al., 2019; Herzing and Johnson, 1997), have also
303 been reported, suggesting genetic diversity alone is not a good proxy for susceptibility to
304 hybridisation.

305

306 To investigate whether interspecific gene flow took place during past periods of low
307 population size, we estimated changes in intraspecific genetic diversity through time (Fig.
308 3B-D). The modeled demographic trajectories, using a Pairwise Sequentially Markovian
309 Coalescent model (PSMC), span the past two million years. We could therefore assess the
310 relationship for the three species pairs, where the putative interval for the cessation of lineage
311 sorting/gene flow was contained within this period: harbour/finless porpoise (Phocoenidae),
312 beluga/narwhal (Monodontidae), and bottlenose/Indo-Pacific bottlenose dolphin
313 (Delphinidae) (Fig. 2).

314

315 In the harbour porpoise, we observe an increase in effective population size (N_e)
316 beginning ~1 Ma, the rate of which increases further ~0.5 Ma (Fig. 3C). The timing of
317 expansion overlaps the period during which lineage sorting/gene flow with the finless
318 porpoise ceased (~1.1 - 0.5 Ma, Fig. 2), suggesting gene flow may have occurred between the
319 two species when population size in the harbour porpoise was lower. We observe a similar
320 pattern in belugas; an increase in N_e ~1 Ma, relatively soon after the proposed cessation of
321 gene flow with narwhals ~1.8 - 1.2 Ma (Fig. 3D). An increase in N_e may coincide with an
322 increase in relative abundance, which would increase the number of potential conspecific
323 mates, and in turn reduce the level of interspecific gene flow. Although we are unable to test
324 the direction and level of gene flow between these species pairs, we expect a relative decline
325 of gene flow into the more abundant species. A relative reduction of such events would in
326 turn lessen genomic signs of interspecific gene flow, despite its occurrence.

327

328 We observe a different pattern in the bottlenose/Indo-Pacific bottlenose dolphins. In
329 the previous examples, we find a relatively low population size when putative gene flow was
330 ongoing, and only in one of the two hybridizing species. In the dolphins, we find a relatively
331 high population size during the period of gene flow in both species; N_e declines ~1 - 0.5 Ma,
332 coinciding with the putative end of gene flow ~1.2 - 0.4 Ma. The decline in N_e could either
333 reflect a decline in abundance, or a loss of connectivity between the two species. In the latter,
334 we expect levels of intraspecific diversity (and thereby inferred N_e) to decline with the
335 cessation of gene flow, even if absolute abundances did not change. This is indeed suggested
336 by our data, which shows both species undergoing the decline simultaneously, indicative of a
337 common cause.

338

339 Seven of the nine Delphinoidea genomes investigated show a similar pattern of a
340 rapid decline in N_e starting ~150 - 100 thousands of years ago (kya) (Fig. 3B-D; the
341 exceptions are Pacific white-sided dolphin and narwhal). This concurrent decline could
342 represent actual population declines across species, or, alternatively, simultaneous reductions
343 in connectivity among populations within each species. Based on similar PSMC analyses, a
344 decline in N_e at this time has also been reported in four baleen whale species (Árnason et al.,
345 2018). Although this could reflect demographic factors, such as the loss of population
346 connectivity, the unique life histories, distributions, and ecology of these cetacean species
347 suggests that decreased population connectivity is unlikely to have occurred simultaneously
348 across all studied species.

349

350 Rather, the species-wide pattern may reflect climate-driven environmental change.
351 The period of 150 - 100 kya overlaps with the onset of the last interglacial, when sea levels
352 increased to levels as high, if not higher, than at present (Polyak et al., 2018), and which may
353 have had a marine-wide effect on population sizes. A similar marine-wide effect has been
354 observed among baleen whales and their prey species in the Southern and North Atlantic
355 Oceans during the Pleistocene-Holocene climate transition (12-7 kya) (Cabrera et al., 2018).
356 These results indicate that past marine-wide environmental shifts have driven changes in
357 population sizes across multiple species.

358
359 Although speculative, our demographic results suggest recent species-wide declines
360 may have facilitated the resurgence of hybridization between the nine Delphinoidea species
361 analysed. If hybridisation did increase, species may already have been sufficiently
362 differentiated that offspring fertility was reduced. Even if offspring were fertile, the high
363 level of differentiation between species may mean hybrids are unable to occupy either
364 parental niche (Skovrind et al., 2019) and have therefore been strongly selected against. A
365 lack of significant contribution from hybrids to the parental gene pools may be why we
366 observe contemporary hybrids, but do not find evidence of this in our analyses.

367

368 **Conclusions**

369

370 Allopatric speciation is generally considered the most common mode of speciation, as
371 the absence of gene flow due to geographical isolation can most easily explain the evolution
372 of ecological, behavioural, morphological, or genetic differences between populations (Norris
373 and Hull, 2012). However, our findings suggest that within Delphinoidea, speciation in the
374 presence of gene flow was commonplace, consistent with sympatric/parapatric speciation, or
375 allopatric speciation and secondary contact.

376

377 The ability for gene flow events to occur long after initial divergence may also
378 explain the presence of contemporaneous hybrids between several species. In parapatric
379 speciation, genetic isolation is achieved relatively early due to geographical and biological
380 isolation, but species develop complete reproductive isolation relatively slowly, through low
381 levels of migration or secondary contact events that allow hybridisation to continue for an
382 extended period of time (Norris and Hull, 2012). The prevalence of this mode of speciation in
383 cetaceans, as suggested by our study and previous genomic analyses (Árnason et al., 2018;
384 Moura et al., 2020), may reflect the low energetic costs of dispersing across large distances in
385 the marine realm (Fish et al., 2008; Williams, 1999) and the relative absence of geographic
386 barriers preventing such dispersal events (Palumbi, 1994). Both factors are believed to be
387 important in facilitating long-distance (including inter-hemispheric and inter-oceanic)
388 movements in many cetacean species (Stone et al., 1990).

389

390 Our study shows that speciation in Delphinoidea was a complex process and involved
391 multiple ecological and evolutionary factors. Our results take a step towards resolving the
392 enormous complexity of speciation, through a multifaceted analysis of nuclear genomes.
393 However, our study also underscores the challenges of precisely interpreting some results,

394 due to the high levels of divergence between the target species. Despite this, we are still able
395 to form hypotheses about general patterns and major processes uncovered in our data, which
396 we hope will be further addressed as additional genomic data and new methodologies for data
397 analysis become available.

398

399 **Methods**

400

401 **Data collection**

402 We downloaded the assembled genomes and raw sequencing reads from nine toothed
403 whales from the superfamily Delphinoidea. The data included five Delphinidae: Pacific
404 white-sided dolphin (NCBI Biosample: SAMN09386610), Indo-Pacific bottlenose dolphin
405 (NCBI Biosample: SAMN06289676), bottlenose dolphin (NCBI Biosample:
406 SAMN09426418), killer whale (NCBI Biosample: SAMN01180276), and long-finned pilot
407 whale (NCBI Biosample: SAMN11083132); two Phocoenidae: harbour porpoise (Autenrieth
408 et al., 2018) and finless porpoise (NCBI Biosample: SAMN02192673); and two
409 Monodontidae: beluga (NCBI Biosample: SAMN06216270) and narwhal (NCBI Biosample:
410 SAMN10519625). To avoid biases that may occur when mapping to an ingroup reference
411 (Westbury et al., 2019), we used the assembled baiji genome (Genbank accession code:
412 GCF_000442215.1) as mapping reference in the gene flow analyses. Delphinoidea and the
413 baiji diverged ~24.6 Ma (95% CI 25.2 - 23.8 Ma) (McGowen et al., 2020).

414

415 **Initial data filtering**

416 To determine which scaffolds were most likely autosomal in origin, we identified
417 putative sex chromosome scaffolds for each genome, and omitted them from further analysis.
418 We found putative sex chromosome scaffolds in all ten genomes by aligning the assemblies
419 to the Cow X (Genbank accession: CM008168.2) and Human Y (Genbank accession:
420 NC_000024.10) chromosomes. Alignments were performed using satsuma synteny v2.1
421 (Grabherr et al., 2010) with default parameters. We also removed scaffolds smaller than 100
422 kb from all downstream analyses.

423

424 **Mapping**

425 We trimmed adapter sequences from all raw reads using skewer v0.2.2 (Jiang et al.,
426 2014). We mapped the trimmed reads to the baiji for downstream gene flow analyses, and to
427 the species-specific reference genome for downstream demographic history and genetic
428 diversity analyses using BWA v0.7.15 (Li and Durbin, 2009) and the mem algorithm. We
429 parsed the output and removed duplicates and reads with a mapping quality lower than 30
430 with SAMtools v1.6 (Li et al., 2009). Mapping statistics can be found in supplementary tables
431 S7 and S8.

432

433 **Sliding-window phylogeny**

434 For the sliding-window phylogenetic analysis, we created fasta files for all individuals
435 mapped to the baiji genome using a consensus base call (-dofasta 2) approach in ANGSD
436 v0.921 (Korneliussen et al., 2014), and specifying the following filters: minimum read depth
437 of 5 (-mininddepth 5), minimum mapping quality of 30 (-minmapq 30), minimum base

438 quality (-minq 30), only consider reads that map to one location uniquely (-uniqueonly 1),
439 and only include reads where both mates map (-only_proper_pairs 1). All resultant fasta files,
440 together with the assembled baiji genome, were aligned, and sites where any individual had
441 more than 50% missing data were filtered before performing maximum likelihood
442 phylogenetic analyses in a non-overlapping sliding-window approach using RAxML v8.2.10
443 (Stamatakis, 2014). We performed this analysis four times independently, specifying a
444 different window size each time (50 kb, 100 kb, 500 kb, and 1 Mb). We used RAxML with
445 default parameters, specifying baiji as the outgroup, and a GTR+G substitution model. We
446 computed the genome-wide majority rule consensus tree for each window size in PHYLIP
447 (Felsenstein, 2005), with branch support represented by the proportion of trees displaying the
448 same topology. We simultaneously visualised all trees of the same sized window using
449 DensiTree (Bouckaert, 2010).

450 We tested whether results may be linked to GC content in the 50kb windows. To do
451 this, we calculated the GC content for each window and binned the windows into three bins:
452 The 33% with the lowest levels of GC content, the 33% with intermediate levels, and the
453 33% with the highest levels of GC content.

454

455 **Quantifying Introgression via Branch Lengths (QuIBL)**

456 To test hypotheses of whether phylogenetic discordance between all possible triplets
457 can be explained by ILS alone, or by a combination of ILS and gene flow, we implemented
458 QuIBL (Edelman et al., 2019) in two different datasets. The first dataset leveraged the results
459 of the above 50 kb-window analysis, by taking every twentieth tree from the 50kb sliding-
460 window analysis and running it through QuIBL. The second dataset was created specifically
461 for this test, and contained topologies generated from 20 kb windows with a 1 Mb slide using
462 the phylogenetic methods mentioned above. We ran QuIBL specifying the baiji as the overall
463 outgroup (totaloutgroup), to test either ILS or ILS with gene flow (numdistributions 2), the
464 number of total EM steps as 50 (numsteps), and a likelihood threshold of 0.01. We
465 determined the significance of gene flow by comparing the BIC1 (ILS alone) and BIC2
466 (assuming ILS and gene flow). When BIC2 was lower than BIC1, with a difference of > 10,
467 we assumed incongruent topologies arose due to both ILS and gene flow. Triplet topologies
468 supporting the species tree, and those that had < 5 alternative topologies were excluded from
469 interpretations.

470

471 **D-statistics**

472 To test for signs of gene flow in the face of incomplete lineage sorting (ILS), we ran
473 D-statistics using all individuals mapped to the baiji genome in ANGSD, using a consensus
474 base call approach (-doabbababa 2), specifying the baiji sequence as the ancestral outgroup
475 sequence, and the same filtering as for the fasta file construction with the addition of setting
476 the block size as 1Mb (-blocksize). Significance of the results was evaluated using a block
477 jackknife approach with the Rscript provided in the ANGSD package. $|Z| > 3$ was deemed
478 significant.

479

480 **D-foil**

481 As D-statistics only tests for the presence and not the direction of gene flow, we ran
482 D-foil (Pease and Hahn, 2015), an extended version of the D-statistics, which is a five-taxon
483 test for gene flow, making use of all four combinations of the potential D-statistics
484 topologies. For this analysis, we used the same fasta files constructed above, which we
485 converted into an mvf file using MVFtools (Pease and Rosenzweig, 2018). We specified the
486 5-taxon [[H1, H2], [H3, H4], baiji], for all possible combinations, following the species tree
487 (McGowen et al., 2020) Fig. 1) and a 100 kb window size. All scaffolds were trimmed to the
488 nearest 100 kb to avoid the inclusion of windows shorter than 100 kb.

489

490 **Mutation rate estimation**

491 For use in the downstream demographic analyses, we computed the mutation rate per
492 generation for each species. To do this, we estimated the pairwise distances between all
493 ingroup species mapped to the baiji, using a consensus base call in ANGSD (-doIBS 2), and
494 applying the same filters as above, with the addition of only considering sites in which all
495 individuals were covered (-minInd). The pairwise distances used in this calculation were
496 those from the closest lineage to the species of interest (Supplementary Tables S9 and S10).
497 The mutation rates per generation were calculated using the resultant pairwise distance as
498 follows: mutation rate = pairwise distance x generation time / 2 x divergence time.
499 Divergence times were taken from the full dataset 10-partition AR (mean) values from
500 McGowen et al. (McGowen et al., 2020) (Supplementary Table S10). Generation times were
501 taken from previously published data (Supplementary Table S11).

502

503 **Cessation of lineage sorting and/or gene flow**

504 To estimate when lineage sorting and/or gene flow may have ceased between each
505 species pair, we used the F1-hybrid PSMC (hPSMC) approach (Cahill et al., 2016). As input
506 we used the haploid consensus sequences mapped to the baiji that were created for the
507 phylogenetic analyses. Despite the possibility of producing consensus sequences when
508 mapping to a conspecific reference genomes, we chose the baiji for all comparisons as
509 previous analyses have shown the choice of reference genome to not influence the results of
510 hPSMC (Westbury et al., 2019). We merged the haploid sequences from each possible
511 species pair into pseudo-diploid sequences using the scripts available in the hPSMC toolsuite.
512 We independently ran each resultant species pair pseudo-diploid sequences through PSMC,
513 specifying atomic intervals 4+25*2+4+6. We plotted the results using the average (i)
514 mutation rate per generation and (ii) generation time for each species pair being tested. From
515 the output of this analysis, we visually estimated the pre-divergence N_e of each hPSMC plot
516 (i.e. N_e prior to the point of asymptotic increase in N_e) to be used as input for downstream
517 simulations. Based on these empirical results, we ran simulations in ms (Hudson, 2002) using
518 the estimated pre-divergence N_e , and various predefined divergence times to find the interval
519 in which gene flow may have ceased between a given species pair. The time intervals and
520 pre-divergence N_e for each species pair used for the simulations can be seen in
521 supplementary table S12. The ms commands were produced using the scripts available in the
522 hPSMC toolsuite. We plotted the simulated and empirical hPSMC results to find the
523 simulations with an asymptotic increase in N_e closest to, but not overlapping with, the
524 empirical data. The predefined divergence times of the simulations showing this pattern

525 within 1.5x and 10x of the pre-divergence N_e were taken as the time interval in which gene
526 flow ceased.

527

528 We repeated the above analysis for three species pairs bottlenose/Indo-Pacific
529 bottlenose dolphins, beluga/narwhal, and beluga/bottlenose dolphin, but with an additional
530 step, where we masked repeat elements of the haploid genomes using bedtools v2.26.0
531 (Quinlan, 2014) and the repeat annotations available on Genbank. Once we masked the repeat
532 elements, we reran the hPSMC analysis as above.

533

534 **Relative divergence times in Delphinidae**

535 To further examine the timing of the ending of lineage sorting and/or gene flow, we
536 performed phylogenetic inferences to uncover the relative divergence times on subsets of
537 genomic loci showing alternative topologies in Delphinidae. For this, we masked repeats in
538 the same fasta files used for our other phylogenetic analyses using the baiji Genbank
539 annotation and bedtools (Quinlan, 2014). We extracted 1 kb windows with a 1 Mb slide from
540 the aligned fasta files and only kept loci containing less than 50% missing data for any
541 individual. We separated our data set into the loci that supported each of four sets of
542 relationships Supplementary Fig. S5. These included loci that supported (i) the consensus
543 species tree ($n = 109$), (ii) the Pacific white-sided dolphin as sister to the killer-whale ($n =$
544 84), (iii) the Pacific white-sided dolphin as sister to the clade of bottlenose dolphins, with the
545 long-finned pilot and killer whales in a monophyletic clade as sisters to this group ($n = 48$),
546 and (iv) the Pacific white-sided dolphin as sister to the long-finned pilot whale ($n = 59$). For
547 each of the four sets, we inferred the relative divergence times across our samples of
548 Delphinidae, also including the beluga and the baiji in the taxon set. We analysed each data
549 set independently, constrained the tree topology to that of the corresponding set of loci, and
550 constrained the age of the root to 1. We performed Bayesian dating using a GTR+ Γ
551 substitution model and an uncorrelated-gamma relaxed clock model in MCMCtree, as
552 implemented in PAML v4.8 (Yang, 2007). The posterior distribution was approximated using
553 Markov chain Monte Carlo (MCMC) sampling, with samples drawn every 10^3 MCMC steps
554 over 10^7 steps, after discarding a burn-in phase of 10^5 steps. Convergence to the stationary
555 distribution was verified by comparing parameter estimates from two independent analyses,
556 and confirming that effective sample sizes were above 200 for all sampled parameters.

557

558 **Heterozygosity**

559 As a proxy for species-level genetic diversity, we estimated autosome-wide
560 heterozygosity for each of the nine Delphinoidea species. We estimated autosomal
561 heterozygosity using allele frequencies (-doSaf 1) in ANGSD (Korneliussen et al., 2014),
562 taking genotype likelihoods into account (-GL 2) and specifying the same filters as for the
563 fasta file construction with the addition of adjusting quality scores around indels (-baq 1), and
564 the subsample filter (-downSample), which was uniquely set for each individual to result in a
565 20x genome-wide coverage, to ensure comparability between genomes of differing coverage.
566 Heterozygosity was computed from the output of this using realSFS from the ANGSD
567 toolsuite and specifying 20 Mb windows of covered sites (-nSites).

568

569 **Demographic reconstruction**

570 To determine the demographic histories of all nine species over a two million year
571 time scale, we ran a Pairwise Sequentially Markovian Coalescent model (PSMC) (Li and
572 Durbin, 2011) on each diploid genome independently. We called diploid genome sequences
573 using SAMtools and BCFtools v1.6 (Narasimhan et al., 2016), specifying a minimum quality
574 score of 20 and minimum coverage of 10. We ran PSMC specifying atomic intervals
575 $4+25*2+4+6$ and performed 100 bootstrap replicates to investigate support for the resultant
576 demographic trajectories. PSMC outputs were plotted using species-specific mutation rates
577 and generation times (Supplementary Table S11).

578

579 **Figure legends:**

580

581 **Figure 1: Sliding-Window Maximum likelihood trees of nine Delphinoidea species and**
582 **the baiji.** Simultaneously plotted trees constructed using non-overlapping sliding windows of
583 (A) 50 kb in length and (B) 1 Mb in length. Black lines show the consensus tree. Grey lines
584 show individual trees. Numbers on branches show the proportion of windows supporting the
585 node. Branches without numbers show 100% support. Baiji, killer whale, Pacific white-sided
586 dolphin, long-finned pilot whale, harbour porpoise, finless whale, beluga, and narwhal
587 silhouettes: Chris huh, license CC-BY-SA-3.0 ([https://creativecommons.org/licenses/by-](https://creativecommons.org/licenses/by-sa/3.0/)
588 [sa/3.0/](https://creativecommons.org/licenses/by-sa/3.0/)). Bottlenose dolphin silhouette: license Public Domain Dedication 1.0.

589

590 **Figure 2: Estimated divergence times (dark colour) and time intervals during which**
591 **gene flow ceased (light colour) between species (A) within families and (B) between**
592 **families.** Estimated time intervals of when gene flow ceased between species pairs are based
593 on hPSMC results and simulated data. Divergence time estimates are taken from the full
594 dataset 10-partition **AR** results of McGowen et al 2020.

595

596 **Figure 3: Autosome-wide heterozygosity and demographic histories over the past two**
597 **million years.** (A) Autosome-wide levels of heterozygosity calculated in 20 Mb windows of
598 consecutive bases. (B-D) Demographic history of all studied species within (B) Delphinidae,
599 (C) Phocoenidae, and (D) Monodontidae, estimated using PSMC. Thick coloured lines show
600 the autosome-wide demographic history. Faded lines show bootstrap support values.

601

602

603

604

605 **Acknowledgements**

606 The work was supported by the Independent Research Fund Denmark | Natural Sciences,
607 Forskningsprojekt 1, grant no. 8021-00218B and the Villum Fonden Young Investigator
608 Programme, grant no. 13151 to EDL. AAC was funded by the Rubicon-NWO grant (project
609 019.183EN.005). We would like to thank all those contributing to the ever-increasing
610 abundance of publicly available genomic resources. Without the availability of such data, our
611 study would not have been possible. We would also like to thank Michael Fontaine,

612 Christelle Fraïsse, Camille Roux, and Andrew Foote for their helpful input to previous
613 versions of this manuscript.

614

615 **Author contributions**

616 Conceptualization, MVW; Formal analysis, MVW, AAC, AR-I, BDC, DAD, SH; Writing –
617 Original Draft MVW; Writing – Review & Editing All authors; Supervision, MVW, EDL;
618 Funding Acquisition, EDL;

619

620 **References:**

- 621 Árnason Ú, Lammers F, Kumar V, Nilsson MA, Janke A. 2018. Whole-genome sequencing
622 of the blue whale and other rorquals finds signatures for introgressive gene flow. *Sci Adv*
623 **4**:eaap9873.
- 624 Autenrieth M, Hartmann S, Lah L, Roos A, Dennis AB, Tiedemann R. 2018. High-quality
625 whole-genome sequence of an abundant Holarctic odontocete, the harbour porpoise
626 (*Phocoena phocoena*). *Mol Ecol Resour* **18**:1469–1481.
- 627 Baird RW, Gorgone AM, McSweeney DJ, Ligon AD, Deakos MH, Webster DL, Schorr GS,
628 Martien KK, Salden DR, Mahaffy SD. 2012. Population structure of island-associated
629 dolphins: Evidence from mitochondrial and microsatellite markers for common
630 bottlenose dolphins (*Tursiops truncatus*) in the main Hawaiian Islands. *Mar Mamm Sci*.
631 Barlow A, Cahill JA, Hartmann S, Theunert C, Xenikoudakis G, Fortes GG, Pajmans JLA,
632 Rabeder G, Frischauf C, Grandal-d'Anglade A, García-Vázquez A, Murtskhvaladze M,
633 Saarma U, Anijalg P, Skrbinšek T, Bertorelle G, Gasparian B, Bar-Oz G, Pinhasi R,
634 Slatkin M, Dalén L, Shapiro B, Hofreiter M. 2018. Partial genomic survival of cave
635 bears in living brown bears. *Nat Ecol Evol* **2**:1563–1570.
- 636 Bierne N, Bonhomme F, David P. 2003. Habitat preference and the marine-speciation
637 paradox. *Proc Biol Sci* **270**:1399–1406.
- 638 Bouckaert RR. 2010. DensiTree: making sense of sets of phylogenetic trees. *Bioinformatics*
639 **26**:1372–1373.
- 640 Butlin RK, Smadja CM. 2018. Coupling, Reinforcement, and Speciation. *Am Nat* **191**:155–
641 172.
- 642 Cabrera AA, Schall E, Bérubé M, Bachmann L, Berrow S, Best PB, Clapham PJ, Cunha HA,
643 Rosa LD, Dias C, Findlay KP, Haug T, Heide-Jørgensen MP, Kovacs KM, Landry S,
644 Larsen F, Lopes XM, Lydersen C, Mattila DK, Oosting T, Pace RM, Papetti C, Paspatis
645 A, Pastene LA, Prieto R, Ramp C, Robbins J, Ryan C, Sears R, Secchi ER, Silva MA,
646 Víkingsson G, Wiig Ø, Øien N, Palsbøll PJ. 2018. Strong and lasting impacts of past
647 global warming on baleen whale and prey abundance. *bioRxiv*.
- 648 Cahill JA, Soares AER, Green RE, Shapiro B. 2016. Inferring species divergence times using
649 pairwise sequential Markovian coalescent modelling and low-coverage genomic data.
650 *Philos Trans R Soc Lond B Biol Sci* **371**. doi:10.1098/rstb.2015.0138
- 651 Campbell CR, Poelstra JW. 2018. What is Speciation Genomics? The roles of ecology, gene
652 flow, and genomic architecture in the formation of species. *Biol J Linn Soc Lond*
653 **124**:561–583.
- 654 Coyne JA, Orr HA. 2004. Speciation. Sinauer Associates Sunderland, MA.
- 655 Crossman CA, Taylor EB, Barrett-Lennard LG. 2016. Hybridization in the Cetacea:
656 widespread occurrence and associated morphological, behavioral, and ecological factors.
657 *Ecol Evol* **6**:1293–1303.
- 658 Edelman NB, Frandsen PB, Miyagi M, Clavijo B, Davey J, Dikow RB, García-Accinelli G,

659 Van Belleghem SM, Patterson N, Neafsey DE, Challis R, Kumar S, Moreira GRP,
660 Salazar C, Chouteau M, Counterman BA, Papa R, Blaxter M, Reed RD, Dasmahapatra
661 KK, Kronforst M, Joron M, Jiggins CD, McMillan WO, Di Palma F, Blumberg AJ,
662 Wakeley J, Jaffe D, Mallet J. 2019. Genomic architecture and introgression shape a
663 butterfly radiation. *Science* **366**:594–599.

664 Edwards CJ, Suchard MA, Lemey P, Welch JJ, Barnes I, Fulton TL, Barnett R, O’Connell
665 TC, Coxon P, Monaghan N, Valdiosera CE, Lorenzen ED, Willerslev E, Baryshnikov
666 GF, Rambaut A, Thomas MG, Bradley DG, Shapiro B. 2011. Ancient hybridization and
667 an Irish origin for the modern polar bear matriline. *Curr Biol* **21**:1251–1258.

668 Espada R, Olaya-Ponzzone L, Haasova L, Martín E, García-Gómez JC. 2019. Hybridization in
669 the wild between *Tursiops truncatus* (Montagu 1821) and *Delphinus delphis* (Linnaeus
670 1758). *PLoS One* **14**:e0215020.

671 Feder JL, Egan SP, Nosil P. 2012. The genomics of speciation-with-gene-flow. *Trends Genet*
672 **28**:342–350.

673 Felsenstein J. 2005. PHYLIP (Phylogeny Inference Package) version 3.6.

674 Fish FE, Howle LE, Murray MM. 2008. Hydrodynamic flow control in marine mammals.
675 *Integr Comp Biol* **48**:788–800.

676 Foote AD, Morin PA. 2015. Sympatric speciation in killer whales? *Heredity* **114**:537–538.

677 Foote AD, Morin PA, Durban JW, Willerslev E. 2011. Out of the Pacific and back again:
678 insights into the matrilineal history of Pacific killer whale ecotypes. *PLoS*.

679 Grabherr MG, Russell P, Meyer M, Mauceli E, Alföldi J, Di Palma F, Lindblad-Toh K. 2010.
680 Genome-wide synteny through highly sensitive sequence alignment: Satsuma.
681 *Bioinformatics* **26**:1145–1151.

682 Gridley T, Elwen SH, Harris G, Moore DM, Hoelzel AR, Lampen F. 2018. Hybridization in
683 bottlenose dolphins—A case study of *Tursiops aduncus* × *T. truncatus* hybrids and
684 successful backcross hybridization events. *PLoS One* **13**:e0201722.

685 Herzing DL, Johnsonz CM. 1997. Interspecific interactions between Atlantic spotted
686 dolphins (*Stenella frontalis*) and bottlenose dolphins (*Tursiops truncatus*) in the
687 Bahamas 1985-1995. *Aquat Mamm*.

688 Hudson RR. 2002. Generating samples under a Wright–Fisher neutral model of genetic
689 variation. *Bioinformatics* **18**:337–338.

690 Jiang H, Lei R, Ding S-W, Zhu S. 2014. Skewer: a fast and accurate adapter trimmer for
691 next-generation sequencing paired-end reads. *BMC Bioinformatics* **15**:182.

692 Korneliussen TS, Albrechtsen A, Nielsen R. 2014. ANGSD: Analysis of Next Generation
693 Sequencing Data. *BMC Bioinformatics* **15**:356.

694 Lartillot N. 2013. Phylogenetic patterns of GC-biased gene conversion in placental mammals
695 and the evolutionary dynamics of recombination landscapes. *Mol Biol Evol* **30**:489–502.

696 Leaché AD, Harris RB, Rannala B, Yang Z. 2014. The influence of gene flow on species tree
697 estimation: a simulation study. *Syst Biol* **63**:17–30.

698 Li H, Durbin R. 2011. Inference of human population history from individual whole-genome
699 sequences. *Nature* **475**:493–496.

700 Li H, Durbin R. 2009. Fast and accurate short read alignment with Burrows–Wheeler
701 transform. *Bioinformatics* **25**:1754–1760.

702 Li H, Handsaker B, Wysoker A, Fennell T, Ruan J, Homer N, Marth G, Abecasis G, Durbin
703 R, 1000 Genome Project Data Processing Subgroup. 2009. The Sequence
704 Alignment/Map format and SAMtools. *Bioinformatics* **25**:2078–2079.

705 Liu S, Lorenzen ED, Fumagalli M, Li B, Harris K, Xiong Z, Zhou L, Korneliussen TS, Somel
706 M, Babbitt C, Wray G, Li J, He W, Wang Z, Fu W, Xiang X, Morgan CC, Doherty A,
707 O’Connell MJ, McInerney JO, Born EW, Dalén L, Dietz R, Orlando L, Sonne C, Zhang
708 G, Nielsen R, Willerslev E, Wang J. 2014. Population genomics reveal recent speciation

709 and rapid evolutionary adaptation in polar bears. *Cell* **157**:785–794.

710 McGowen MR, Tsagkogeorga G, Álvarez-Carretero S, Dos Reis M, Struebig M, Deaville R,
711 Jepson PD, Jarman S, Polanowski A, Morin PA, Rossiter SJ. 2020. Phylogenomic
712 Resolution of the Cetacean Tree of Life Using Target Sequence Capture. *Syst Biol*
713 **69**:479–501.

714 Mendes FK, Hahn MW. 2016. Gene Tree Discordance Causes Apparent Substitution Rate
715 Variation. *Syst Biol* **65**:711–721.

716 Miralles L, Oremus M, Silva MA, Planes S, Garcia-Vazquez E. 2016. Interspecific
717 Hybridization in Pilot Whales and Asymmetric Genetic Introgression in Northern
718 Globicephala melas under the Scenario of Global Warming. *PLoS One* **11**:e0160080.

719 Miyazaki N, Hirosaki Y, Kinuta T, Omura H. 1992. Osteological study of a hybrid between
720 Tursiops truncatus and Grampus griseus. *Bull Natl Mus Nat Sci Ser B Bot* **18**:79–94.

721 Moodley Y, Westbury MV, Russo I-RM, Gopalakrishnan S, Rakotoarivelo A, Olsen R-A,
722 Prost S, Tunstall T, Ryder OA, Dalén L, Bruford MW. 2020. Interspecific gene flow and
723 the evolution of specialisation in black and white rhinoceros. *Mol Biol Evol*.
724 doi:10.1093/molbev/msaa148

725 Moura AE, Kenny JG, Chaudhuri RR, Hughes MA. 2015. Phylogenomics of the killer whale
726 indicates ecotype divergence in sympatry. *Heredity* **114**:48–55.

727 Moura AE, Shreves K, Pilot M, Andrews KR, Moore DM, Kishida T, Möller L, Natoli A,
728 Gaspari S, McGowen M, Chen I, Gray H, Gore M, Culloch RM, Kiani MS, Willson MS,
729 Bulushi A, Collins T, Baldwin R, Willson A, Minton G, Ponnampalam L, Hoelzel AR.
730 2020. Phylogenomics of the genus *Tursiops* and closely related Delphininae reveals
731 extensive reticulation among lineages and provides inference about eco-evolutionary
732 drivers. *Mol Phylogenet Evol* **146**:106756.

733 Narasimhan V, Danecek P, Scally A, Xue Y, Tyler-Smith C, Durbin R. 2016. BCFtools/RoH:
734 a hidden Markov model approach for detecting autozygosity from next-generation
735 sequencing data. *Bioinformatics* **32**:1749–1751.

736 Norris RD, Hull PM. 2012. The temporal dimension of marine speciation. *Evol Ecol* **26**:393–
737 415.

738 Palumbi SR. 1994. Genetic divergence, reproductive isolation, and marine speciation. *Annu*
739 *Rev Ecol Syst* **25**:547–572.

740 Pamilo P, Nei M. 1988. Relationships between gene trees and species trees. *Mol Biol Evol*
741 **5**:568–583.

742 Pease JB, Hahn MW. 2015. Detection and Polarization of Introgression in a Five-Taxon
743 Phylogeny. *Syst Biol* **64**:651–662.

744 Pease JB, Rosenzweig BK. 2018. Encoding Data Using Biological Principles: The
745 Multisample Variant Format for Phylogenomics and Population Genomics. *IEEE/ACM*
746 *Trans Comput Biol Bioinform* **15**:1231–1238.

747 Polyak VJ, Onac BP, Fornós JJ, Hay C, Asmerom Y, Dorale JA, Ginés J, Tuccimei P, Ginés
748 A. 2018. A highly resolved record of relative sea level in the western Mediterranean Sea
749 during the last interglacial period. *Nat Geosci* **11**:860–864.

750 Quinlan AR. 2014. BEDTools: The Swiss-Army Tool for Genome Feature Analysis. *Curr*
751 *Protoc Bioinformatics* **47**:11.12.1–34.

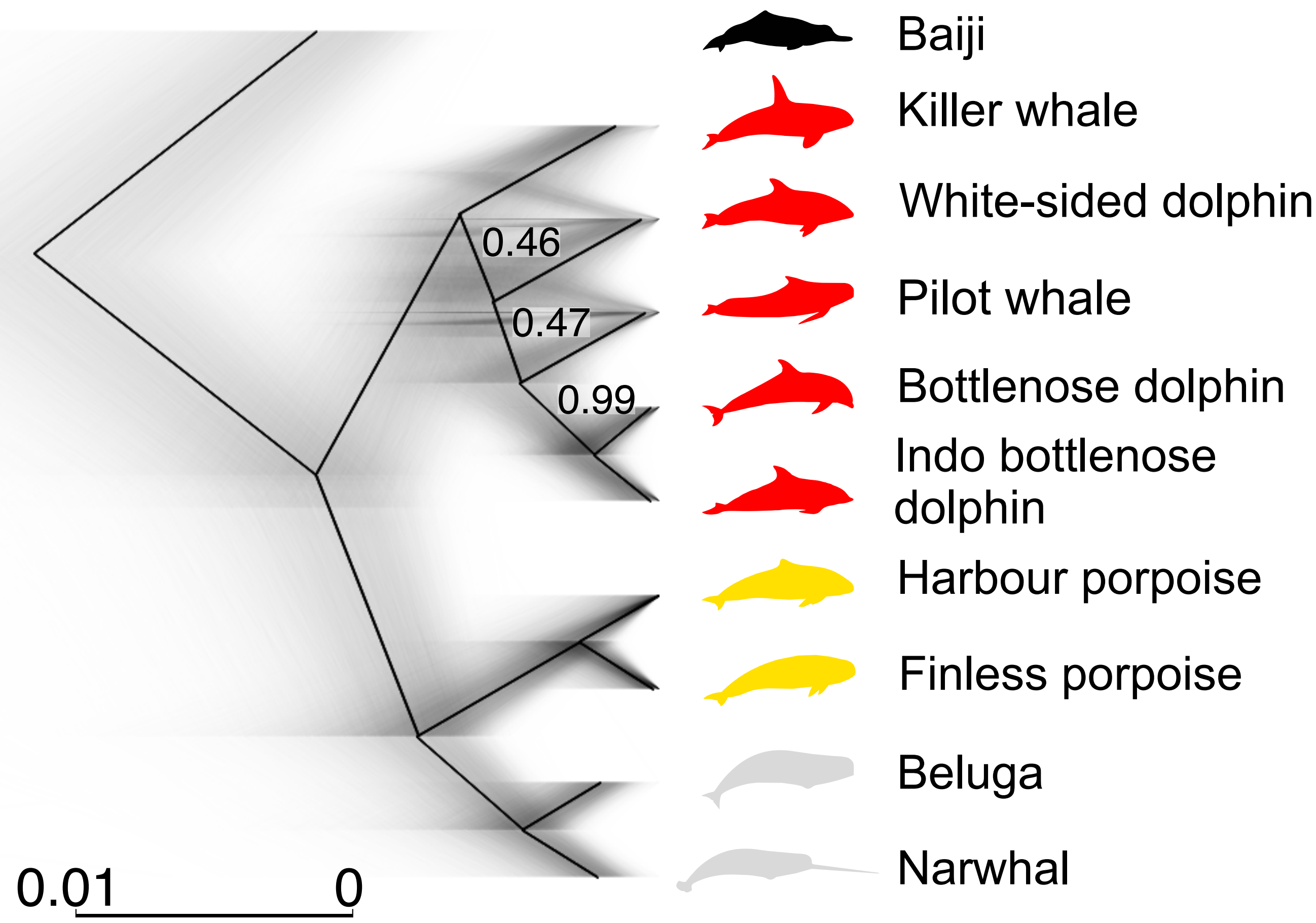
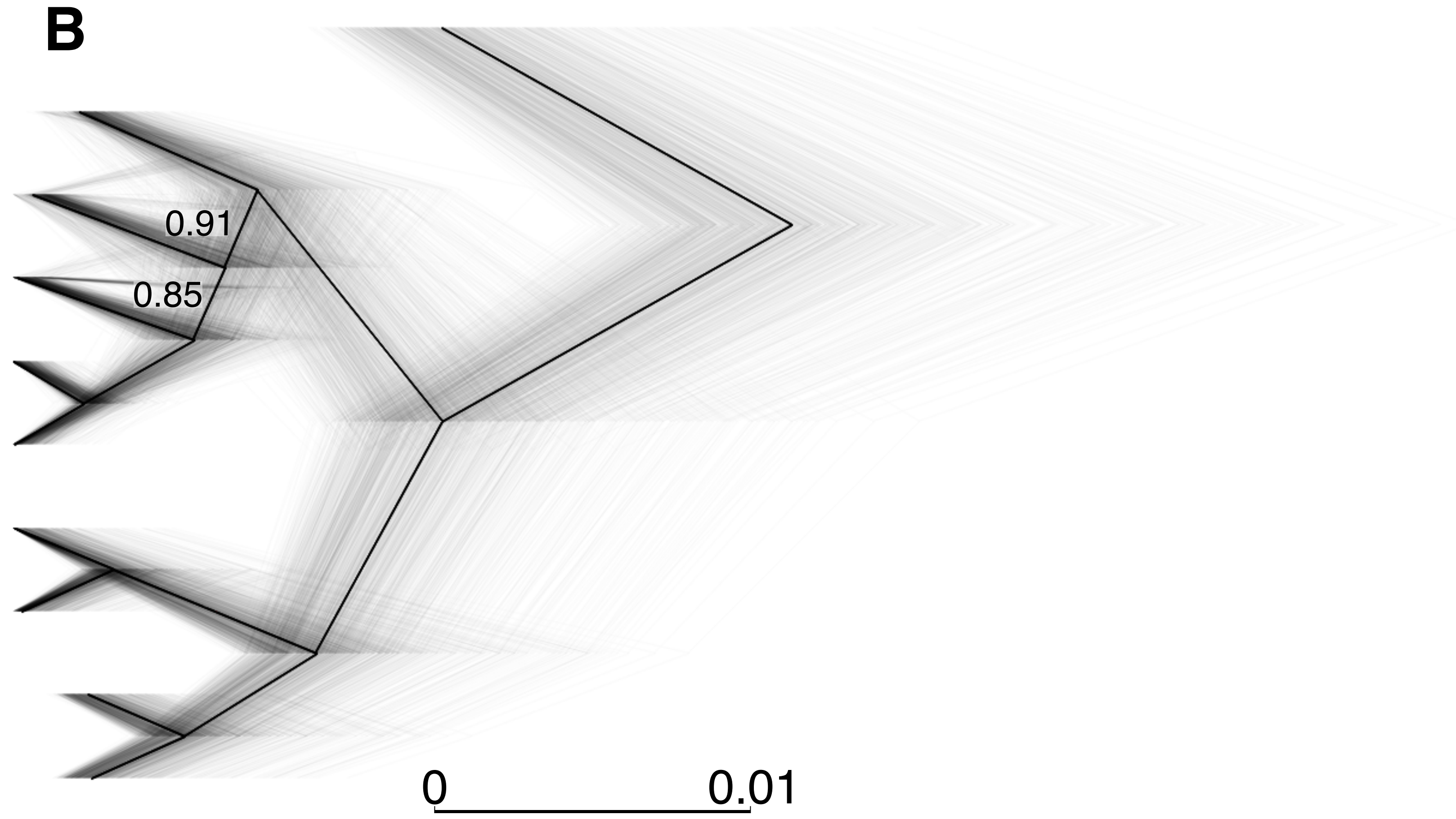
752 Silva JM, Silva FJL, Sazima I. 2005. Two presumed interspecific hybrids in the genus
753 *Stenella* (Delphinidae) in the Tropical West Atlantic. *Aquat Mamm* **31**:468.

754 Skovrind M, Castruita JAS, Haile J, Treadaway EC, Gopalakrishnan S, Westbury MV,
755 Heide-Jørgensen MP, Szpak P, Lorenzen ED. 2019. Hybridization between two high
756 Arctic cetaceans confirmed by genomic analysis. *Sci Rep* **9**:7729.

757 Slatkin M, Pollack JL. 2008. Subdivision in an ancestral species creates asymmetry in gene
758 trees. *Mol Biol Evol* **25**:2241–2246.

- 759 Stamatakis A. 2014. RAxML version 8: a tool for phylogenetic analysis and post-analysis of
760 large phylogenies. *Bioinformatics* **30**:1312–1313.
- 761 Steeman ME, Hebsgaard MB, Fordyce RE, Ho SYW, Rabosky DL, Nielsen R, Rahbek C,
762 Glenner H, Sørensen MV, Willerslev E. 2009. Radiation of extant cetaceans driven by
763 restructuring of the oceans. *Syst Biol* **58**:573–585.
- 764 Stone G, Florez-Gonzalez L, Katona S. 1990. Whale migration record. *Nature* **346**:705–705.
- 765 Turelli M, Barton NH, Coyne JA. 2001. Theory and speciation. *Trends Ecol Evol* **16**:330–
766 343.
- 767 Westbury MV, Hartmann S, Barlow A, Preick M, Ridush B, Nagel D, Rathgeber T, Ziegler
768 R, Baryshnikov G, Sheng G, Ludwig A, Wiesel I, Dalen L, Bibi F, Werdelin L, Heller
769 R, Hofreiter M. 2020. Hyena paleogenomes reveal a complex evolutionary history of
770 cross-continental gene flow between spotted and cave hyena. *Science Advances*
771 **6**:eaay0456.
- 772 Westbury MV, Petersen B, Lorenzen ED. 2019. Genomic analyses reveal an absence of
773 contemporary introgressive admixture between fin whales and blue whales, despite
774 known hybrids. *PLoS One* **14**:e0222004.
- 775 Williams TM. 1999. The evolution of cost efficient swimming in marine mammals: limits to
776 energetic optimization. *Philosophical Transactions of the Royal Society of London*
777 *Series B: Biological Sciences* **354**:193–201.
- 778 Willis PM, Crespi BJ, Dill LM, Baird RW, Hanson MB. 2004. Natural hybridization between
779 Dall's porpoises (*Phocoenoides dalli*) and harbour porpoises (*Phocoena phocoena*). *Can*
780 *J Zool* **82**:828–834.
- 781 Yang Z. 2007. PAML 4: phylogenetic analysis by maximum likelihood. *Mol Biol Evol*
782 **24**:1586–1591.
- 783 Zheng Y, Janke A. 2018. Gene flow analysis method, the D-statistic, is robust in a wide
784 parameter space. *BMC Bioinformatics* **19**:10.

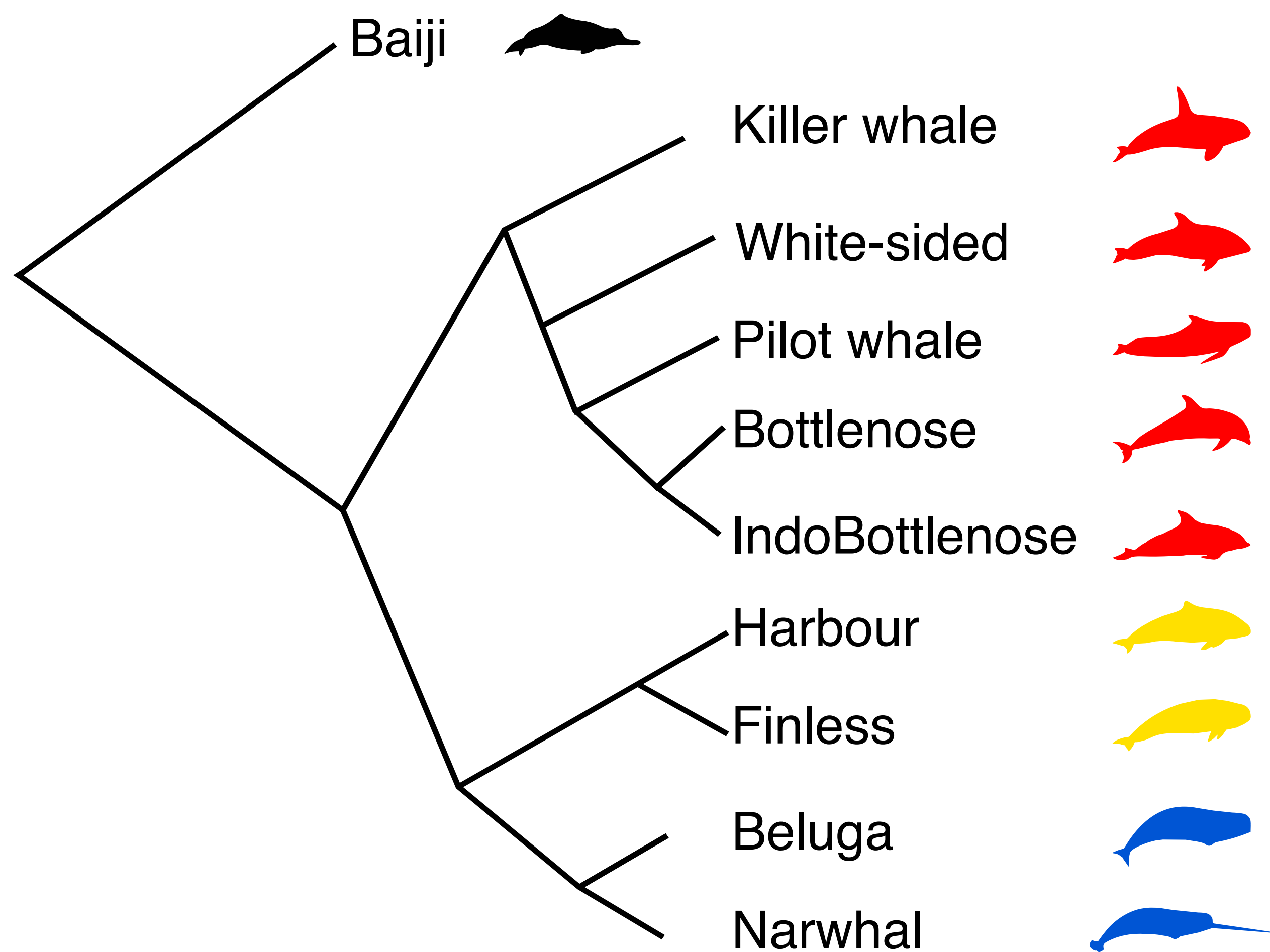
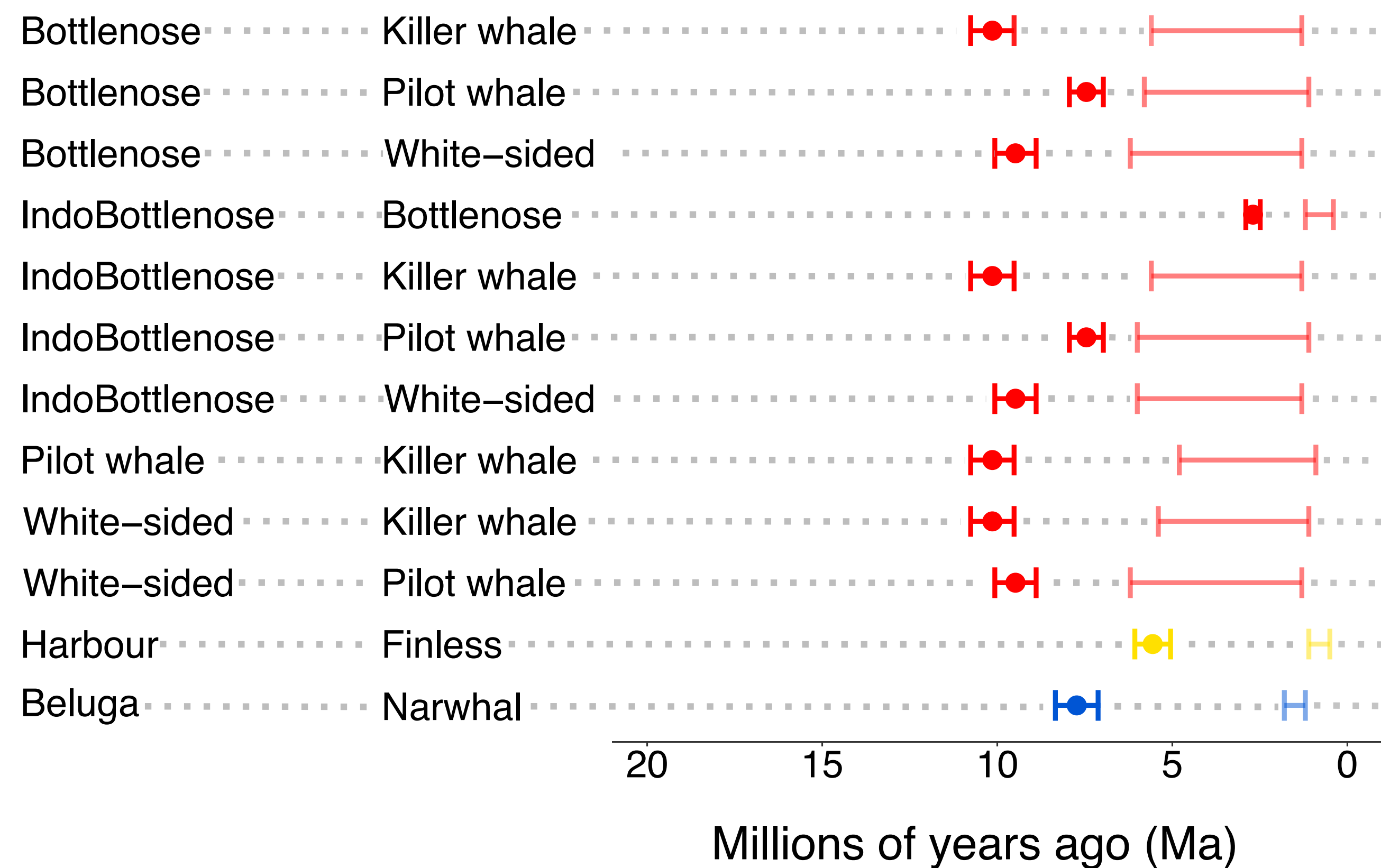
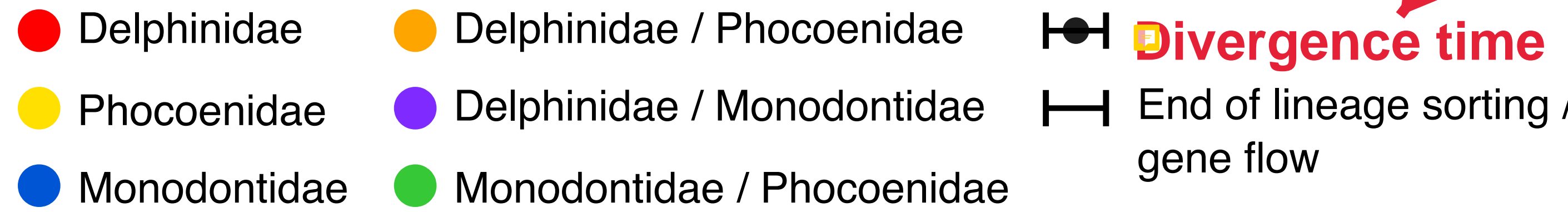
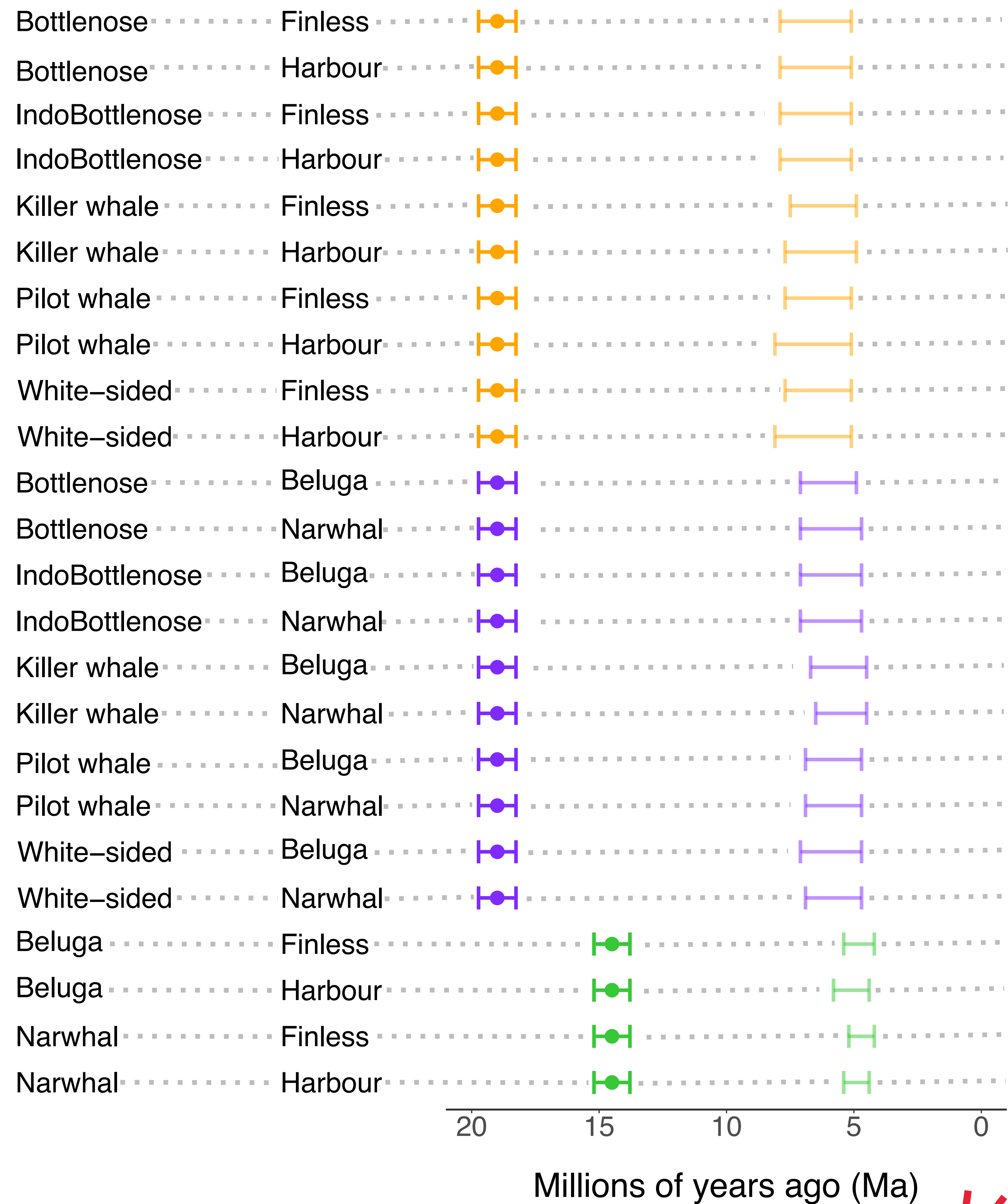
785

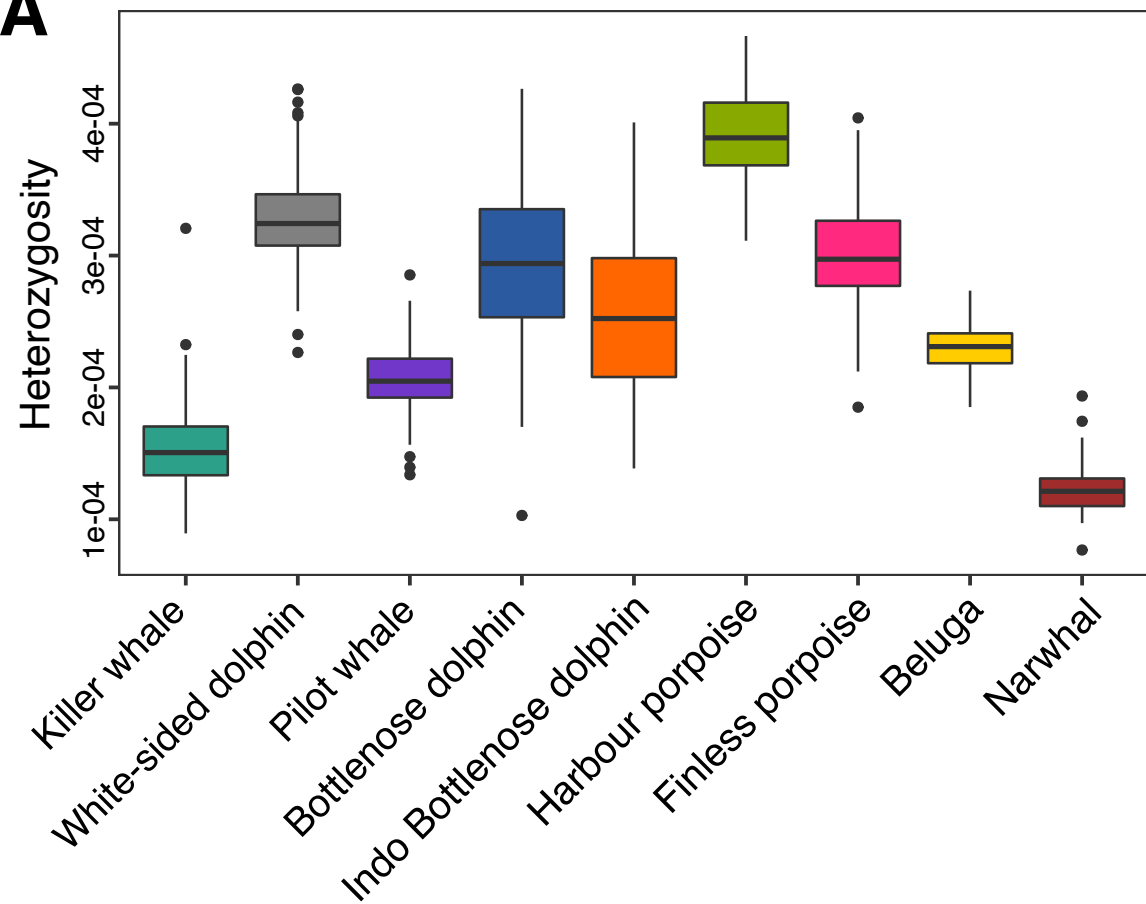
A**B**

0.01 0

0 0.01

● Outgroup ● Delphinidae ● Phocoenidae ● Monodontidae

A**B****Between families**

A**Delphinidae**

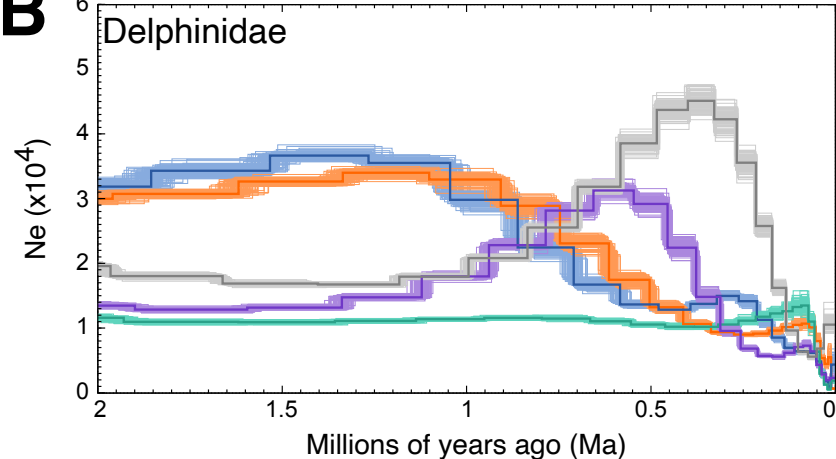
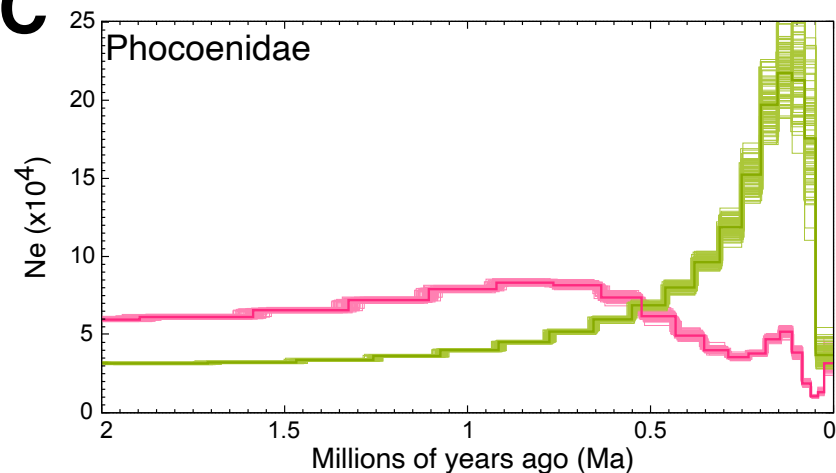
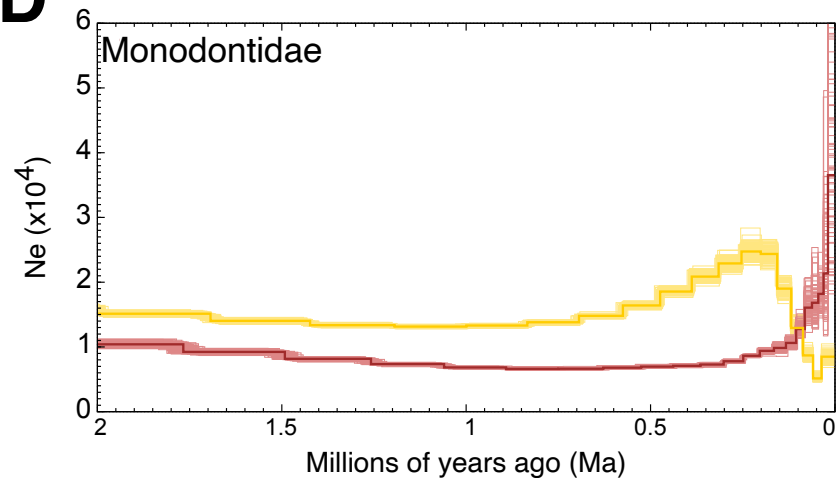
-  Killer whale
-  White-sided dolphin
-  Pilot whale
-  Bottlenose dolphin
-  Indo bottlenose dolphin

Phocoenidae

-  Harbour porpoise
-  Finless porpoise

Monodontidae

-  Beluga
-  Narwhal

B**C****D**

Supplementary information

Supplementary table S1: Proportions of the most frequent five topologies based on window sizes. NA - not in the five most frequent for that window size. Whitesided - Pacific white-sided dolphin, Pilotwhale - long-finned pilot whale, IndoBottlenose - Indo-Pacific bottlenose dolphin, Bottlenose - bottlenose dolphin, Killerwhale - killer whale, Beluga - beluga, Narwhal - narwhal, Harbour - harbour porpoise, Finless - finless porpoise, Baiji - Baiji (outgroup).

50 kb	100 kb	500 kb	1 Mb	Topology
0.24	0.32	0.64	0.79	((((Whitesided,(Pilotwhale,(IndoBottlenose,Bottlenose))),Killerwhale)),((Beluga,Narwhal),(Harbour,Finless))),Baiji);
0.14	0.14	0.09	0.05	((((Pilotwhale,(IndoBottlenose,Bottlenose)),(Whitesided,Killerwhale)),((Beluga,Narwhal),(Harbour,Finless))),Baiji);
0.13	0.14	0.14	0.10	((((Pilotwhale,(Whitesided,(IndoBottlenose,Bottlenose))),Killerwhale)),((Beluga,Narwhal),(Harbour,Finless))),Baiji);
0.09	0.08	0.04	0.02	((((Pilotwhale,Whitesided),(IndoBottlenose,Bottlenose)),Killerwhale)),((Beluga,Narwhal),(Harbour,Finless))),Baiji);
0.08	NA	NA	NA	((((Killerwhale,(Pilotwhale,(IndoBottlenose,Bottlenose))),Whitesided)),((Beluga,Narwhal),(Harbour,Finless))),Baiji);
NA	0.07	0.03	0.02	((((Whitesided,((Pilotwhale,(IndoBottlenose,Bottlenose))),Killerwhale)),((Beluga,Narwhal),(Harbour,Finless))),Baiji);
0.69	0.76	0.94	0.98	Top 5 topologies combined

Supplementary table S2: Proportions of the most frequent five topologies based on GC content and a window size of 50 kb. NA - not in the five most frequent for that window size. Whitesided - Pacific white-sided dolphin, Pilotwhale - long-finned pilot whale, IndoBottlenose - Indo-Pacific bottlenose dolphin, Bottlenose - bottlenose dolphin, Killerwhale - killer whale, Beluga - beluga, Narwhal - narwhal, Harbour - harbour porpoise, Finless - finless porpoise, Baiji - Baiji (outgroup).

Low GC	Medium GC	High GC	Topology
2814	3395	4227	((((Killerwhale,(Whitesided,((IndoBottlenose,Bottlenose),Pilotwhale))),((Beluga,Narwhal),(Harbour,Finless))),Baiji);
2023	2107	2085	((((Pilotwhale,(IndoBottlenose,Bottlenose)),(Whitesided,Killerwhale)),((Beluga,Narwhal),(Harbour,Finless))),Baiji);
1740	1898	1976	((((Pilotwhale,(Whitesided,(IndoBottlenose,Bottlenose))),Killerwhale)),((Beluga,Narwhal),(Harbour,Finless))),Baiji);
1287	1289	1317	((((Pilotwhale,Whitesided),(IndoBottlenose,Bottlenose)),Killerwhale)),((Beluga,Narwhal),(Harbour,Finless))),Baiji);
1152	NA	NA	((((Whitesided,(IndoBottlenose,Bottlenose)),(Pilotwhale,Killerwhale)),((Beluga,Narwhal),(Harbour,Finless))),Baiji);
NA	1190	1149	((((Whitesided,((Pilotwhale,(IndoBottlenose,Bottlenose))),Killerwhale)),((Beluga,Narwhal),(Harbour,Finless))),Baiji);

Supplementary table S3: QuIBL results when using every twentieth tree from the 50 kb sliding window analysis - attached as spreadsheet.

Supplementary table S4: QuIBL results from trees constructed using 20 kb windows with a 1 Mb slide - attached as spreadsheet.

Supplementary table S5: D-statistics results for all triplet combinations phylogenetically concurrent with our results shown in Figure 1. Baiji was used as the outgroup/ancestral sequence. A non-significant result ($|Z| < 3$) is indicated in bold. Colours indicate the family of the given individual. Red = Delphinidae, yellow = Phocoenidae, blue = Monodontidae.

H1	H2	H3	nABBA	nBABA	D-score	Z-score
Bottlenose	IndoBottlenose	Killer whale	597,251	554,780	0.037	23.26
Bottlenose	IndoBottlenose	Pilotwhale	748,948	691,844	0.040	24.13
Bottlenose	IndoBottlenose	Whitesided	721,498	665,420	0.040	25.20
Pilotwhale	Whitesided	Killer whale	2,224,888	2,119,068	0.024	11.77
Pilotwhale	Bottlenose	Killer whale	1,998,297	1,795,444	0.053	26.15
Pilotwhale	IndoBottlenose	Killer whale	2,004,478	1,757,429	0.066	31.95
Pilotwhale	Bottlenose	Whitesided	2,490,189	2,051,579	0.097	42.67
Pilotwhale	IndoBottlenose	Whitesided	2,508,755	2,007,966	0.111	48.64
Whitesided	Bottlenose	Killer whale	2,111,742	2,014,525	0.024	11.88
Whitesided	IndoBottlenose	Killer whale	2,117,925	1,975,800	0.035	17.25
Killer whale	Pilotwhale	Finless	928,942	840,273	0.050	51.99
Killer whale	Whitesided	Finless	924,323	829,525	0.054	56.12
Killer whale	Pilotwhale	Harbour porpoise	959,748	851,885	0.060	60.74
Killer whale	Whitesided	Harbour porpoise	956,686	840,318	0.065	65.46
Killer whale	Bottlenose	Finless	942,684	757,495	0.109	107.12
Killer whale	Bottlenose	Harbour porpoise	974,032	767,636	0.119	116.98
Killer whale	IndoBottlenose	Finless	943,526	728,185	0.129	120.99
Killer whale	IndoBottlenose	Harbour porpoise	974,967	739,024	0.138	130.60
Pilotwhale	Whitesided	Finless	861,276	855,083	0.004	4.41
Pilotwhale	Whitesided	Harbour porpoise	892,930	884,620	0.005	5.64
Pilotwhale	Bottlenose	Finless	828,193	724,397	0.067	73.75
Pilotwhale	Bottlenose	Harbour porpoise	857,823	749,827	0.067	76.38
Pilotwhale	IndoBottlenose	Finless	829,393	692,413	0.090	97.23
Pilotwhale	IndoBottlenose	Harbour porpoise	859,146	718,044	0.089	98.69

Whitesided	Bottlenose	Harbour porpoise	887,876	787,914	0.060	68.88
Whitesided	Bottlenose	Finless	857,483	760,224	0.060	69.75
Whitesided	IndoBottlenose	Harbour porpoise	888,872	755,955	0.081	92.25
Whitesided	IndoBottlenose	Finless	858,523	727,924	0.082	92.84
Bottlenose	IndoBottlenose	Narwhal	414,272	380,995	0.042	33.84
Bottlenose	IndoBottlenose	Beluga	434,366	396,566	0.045	37.67
Killer whale	Pilotwhale	Narwhal	955,756	837,598	0.066	61.58
Killer whale	Pilotwhale	Beluga	984,462	854,528	0.071	65.67
Killer whale	Whitesided	Narwhal	953,496	826,881	0.071	66.17
Killer whale	Whitesided	Beluga	982,162	844,661	0.075	67.95
Killer whale	Bottlenose	Narwhal	971,164	751,458	0.128	111.86
Killer whale	Bottlenose	Beluga	1,001,546	767,422	0.132	113.69
Killer whale	IndoBottlenose	Narwhal	974,507	722,249	0.149	126.51
Killer whale	IndoBottlenose	Beluga	1,007,582	736,424	0.155	128.87
Pilotwhale	Whitesided	Beluga	918,941	911,423	0.004	4.93
Pilotwhale	Whitesided	Narwhal	891,298	883,114	0.005	5.61
Pilotwhale	Bottlenose	Narwhal	859,652	743,735	0.072	78.60
Pilotwhale	Bottlenose	Beluga	887,196	766,562	0.073	81.55
Pilotwhale	IndoBottlenose	Narwhal	863,608	710,777	0.097	103.83
Pilotwhale	IndoBottlenose	Beluga	895,023	731,826	0.100	105.92
Whitesided	Bottlenose	Narwhal	888,390	780,573	0.065	74.77
Whitesided	Bottlenose	Beluga	917,400	804,237	0.066	76.44
Whitesided	IndoBottlenose	Narwhal	892,496	747,539	0.088	97.69
Whitesided	IndoBottlenose	Beluga	925,091	769,228	0.092	102.86
Finless	Harbour porpoise	Narwhal	452,411	450,657	0.002	1.59
Harbour porpoise	Finless	Beluga	570,767	552,830	0.016	13.47
Narwhal	Beluga	Harbour porpoise	532,605	502,660	0.029	25.72
Narwhal	Beluga	Finless	514,273	466,273	0.049	41.75
Finless	Narwhal	Killer whale	973,140	885,678	0.047	47.30
Finless	Narwhal	Bottlenose	1,077,206	966,370	0.054	55.93
Finless	Narwhal	IndoBottlenose	1,080,812	970,600	0.054	56.63
Finless	Narwhal	Pilotwhale	1,059,846	950,178	0.055	57.27
Finless	Beluga	Killer whale	989,901	875,364	0.061	57.51

Finless	Narwhal	Whitesided	1,062,632	951,040	0.055	57.94
Finless	Beluga	Bottlenose	1,103,352	951,967	0.074	68.54
Finless	Beluga	Pilotwhale	1,084,679	936,511	0.073	68.84
Finless	Beluga	IndoBottlenose	1,109,158	955,589	0.074	69.72
Finless	Beluga	Whitesided	1,087,277	938,148	0.074	69.88
Harbour porpoise	Narwhal	Killer whale	1,004,793	891,909	0.060	59.43
Harbour porpoise	Beluga	Killer whale	1,028,676	885,849	0.075	69.85
Harbour porpoise	Narwhal	Pilotwhale	1,124,641	974,232	0.072	75.43
Harbour porpoise	Narwhal	Bottlenose	1,145,470	990,640	0.072	75.66
Harbour porpoise	Narwhal	Whitesided	1,127,578	976,951	0.072	75.84
Harbour porpoise	Narwhal	IndoBottlenose	1,153,263	994,022	0.074	78.93
Harbour porpoise	Beluga	Pilotwhale	1,163,136	965,266	0.093	88.73
Harbour porpoise	Beluga	Whitesided	1,165,862	968,086	0.093	89.42
Harbour porpoise	Beluga	Bottlenose	1,185,612	981,030	0.094	89.66
Harbour porpoise	Beluga	IndoBottlenose	1,197,547	984,311	0.098	93.10

Supplementary table S6: 100kb non-overlapping sliding window D-foil results for all quadruplet combinations [[H1,H2][H3,H4]] phylogenetically concurrent with our results shown in figure 1. Baiji was used as the outgroup/ancestral sequence. - attached as a spreadsheet

Supplementary table S7: Mapping statistics of each Delphinoidea species used in this study when specifying the reference genome as the baiji assembly.

Common name	Raw read pairs	Mapped reads	Coverage	Bp-mapped
Beluga	466,374,135	476,814,543	31.44	69,807,010,359
Bottlenose dolphin	578,690,171	732,418,659	47.61	105,524,983,813
Harbour porpoise	289,063,910	418,431,029	23.17	50,830,083,145
Indo-Pacific bottlenose dolphin	466,306,082	551,837,703	35.62	78,749,625,267
Indo-Pacific finless porpoise	523,612,238	557,766,873	24.96	54,450,935,944
Killer whale	1,467,089,287	1,047,260,000	39.53	88,692,400,000
Long-finned pilot whale	428,064,233	504,482,080	28.61	63,276,638,573
Narwhal	384,563,392	468,429,237	31.09	68,247,058,370
Pacific white-sided dolphin	453,348,710	499,704,592	28.83	63,800,396,300

Supplementary table S8: Mapping statistics of each Delphinoidea species used in this study when specifying the reference genome as a conspecific assembly.

Common name	Raw read pairs	Mapped reads	Coverage	Bp-mapped
Beluga	466,374,135	531,535,936	34.47	79,218,898,913
Bottlenose dolphin	578,690,171	779,210,277	54.03	114,530,169,747
Harbour porpoise	289,063,910	431,762,883	23.74	52,067,455,809
Indo-Pacific bottlenose dolphin	466,306,082	587,440,922	37.88	85,032,333,848
Indo-Pacific finless porpoise	523,612,238	620,580,505	27.33	61,286,732,910
Killer whale	1,467,089,287	1,213,221,913	44.93	100,903,316,971
Long-finned pilot whale	428,064,233	598,612,204	32.79	75,639,560,432
Narwhal	384,563,392	529,082,769	33.85	78,238,763,386
Pacific white-sided dolphin	453,348,710	592,814,373	33.02	76,299,243,217

Supplementary table S9: Genome-wide pairwise distance matrix of the nine Delphinoidea included in this study. Bottlenose = bottlenose dolphin, Finless = finless porpoise, Harbour = harbour porpoise, Indobottle = Indo-Pacific bottlenose dolphin, Killer = killer whale, Pilot = pilot whale, White = Pacific white-sided dolphin.

Beluga	0.0000	0.0211	0.0151	0.0153	0.0211	0.0205	0.0056	0.0210	0.0209
Bottlenose	0.0211	0.0000	0.0230	0.0231	0.0040	0.0113	0.0210	0.0102	0.0107
Finless	0.0151	0.0230	0.0000	0.0056	0.0230	0.0224	0.0151	0.0229	0.0228
Harbour	0.0153	0.0231	0.0056	0.0000	0.0231	0.0225	0.0152	0.0231	0.0230
Indobottle	0.0211	0.0040	0.0230	0.0231	0.0000	0.0113	0.0210	0.0102	0.0107
Killer	0.0205	0.0113	0.0224	0.0225	0.0113	0.0000	0.0204	0.0113	0.0112
Narwhal	0.0056	0.0210	0.0151	0.0152	0.0210	0.0204	0.0000	0.0209	0.0208
Pilot	0.0210	0.0102	0.0229	0.0231	0.0102	0.0113	0.0209	0.0000	0.0109
White	0.0209	0.0107	0.0228	0.0230	0.0107	0.0112	0.0208	0.0109	0.0000

Supplementary table S10: Metrics used to calculate the mutation rate per year with the equation mutation rate = divergence time / 2x genetic distance. Mean divergences were taken from the full dataset 10-partition AR from McGowen et al 2020 (McGowen et al., 2020) and average genetic distances were calculated from the results shown in supplementary table S5.

Species	Closest relative	Divergence (Ma)	Distance	Mutation rate per year
Beluga	Narwhal	7.72	0.0056	3.63×10^{-10}
Killer whale	Delphinidae	10.16	0.0113	5.56×10^{-10}
Bottlenose dolphin	Indo-Pacific bottlenose dolphin	2.69	0.0040	7.51×10^{-10}
Harbour porpoise	Finless porpoise	5.36	0.0056	5.25×10^{-10}
Long-finned pilot whale	<i>Tursiops</i> spp.	7.46	0.0102	6.83×10^{-10}
Pacific white-sided dolphin	<i>Tursiops</i> + <i>Globicephala</i>	9.48	0.0108	5.69×10^{-10}

Supplementary table S11: Generation times, generational mutation rates and references for the generation times for each of the nine Delphinoidea species used in this study.

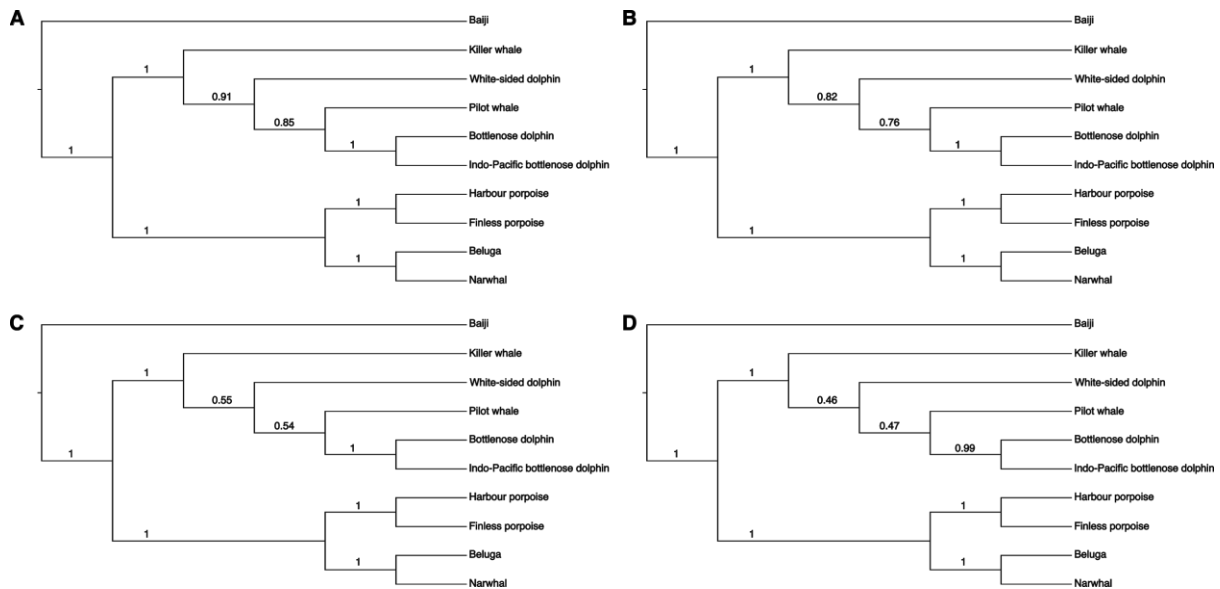
Common name	Generation time	Generational mutation rate	Generation time reference	Bp-mapped
Beluga	32	1.16×10^{-8}	(Garde et al., 2015)	79,218,898,913
Bottlenose dolphin	21	1.58×10^{-8}	(Taylor et al., 2007)	114,530,169,747
Harbour porpoise	10	5.25×10^{-9}	(Birkun and Frantzis, 2008)	52,067,455,809
Indo-Pacific bottlenose dolphin	21	1.58×10^{-8}	(Taylor et al., 2007)	85,032,333,848
Indo-Pacific finless porpoise	8	4.20×10^{-9}	(Zhou et al., 2018)	61,286,732,910
Killer whale	26	1.43×10^{-8}	(Foote et al., 2016)	100,903,316,971
Long-finned pilot whale	24	1.64×10^{-8}	(Taylor et al., 2007)	75,639,560,432
Narwhal	30	1.09×10^{-8}	(Garde et al., 2015)	78,238,763,386
Pacific white-sided dolphin	21	1.21×10^{-8}	(Taylor et al., 2007)	76,299,243,217

Supplementary table S12: The pre-divergence N_e , divergence time intervals, and the increments specified for each of the species pair used for the simulations to compare against the hPSMC results.

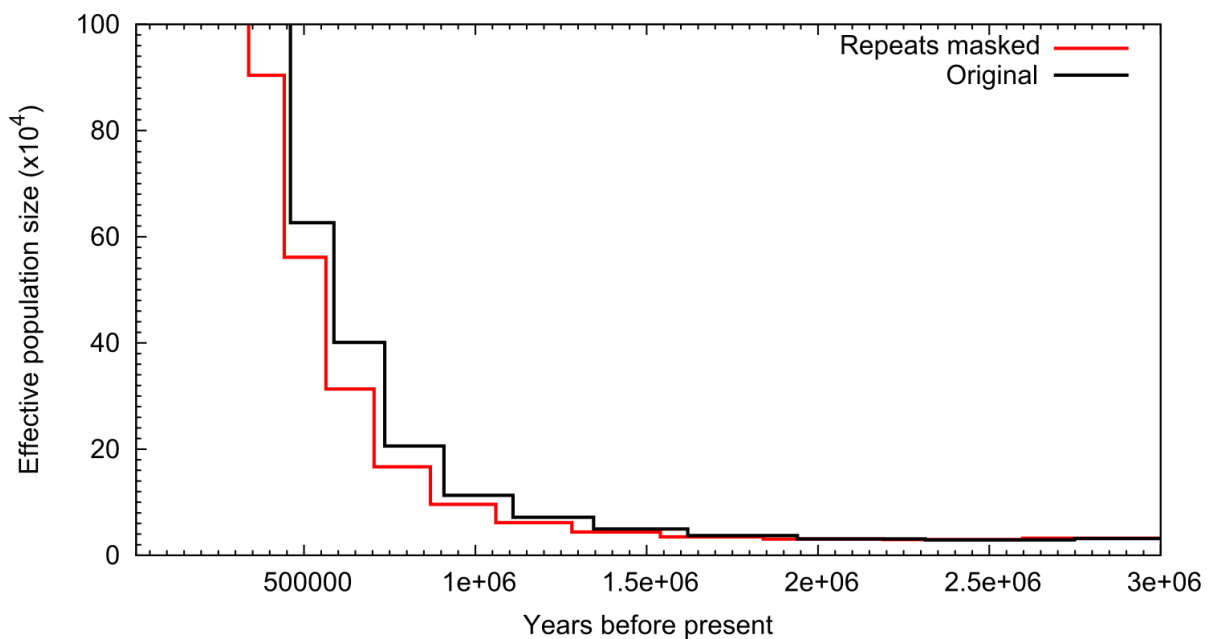
Species pair	Pre-divergence N_e	Range (Ma)	Increments (years)
Beluga whale + Narwhal	30,000	1-2	100,000
Beluga whale + Finless porpoise	60,000	3-7	200,000
Beluga whale + Harbour porpoise	60,000	3-7	200,000
Narwhal + Finless porpoise	60,000	3-7	200,000
Narwhal + Harbour porpoise	60,000	3-7	200,000
Beluga whale + Bottlenose dolphin	105,000	3.9-8.5	200,000
Beluga whale + Indo-Pacific bottlenose dolphin	105,000	3.9-8.5	200,000
Narwhal + Bottlenose dolphin	105,000	3.9-8.5	200,000
Narwhal + Indo-Pacific bottlenose dolphin	105,000	3.9-8.5	200,000
Narwhal + Killer whale	105,000	3.9-8.5	200,000
Narwhal + Long-finned pilot whale	105,000	3.9-8.5	200,000
Narwhal + Pacific white-sided dolphin	105,000	3.9-8.5	200,000
Beluga whale + Killer whale	105,000	3.9-8.5	200,000
Beluga whale + Long-finned pilot whale	105,000	3.9-8.5	200,000
Beluga whale + Pacific white-sided dolphin	105,000	3.9-8.5	200,000
Harbour porpoise + Bottlenose dolphin	105,000	3.9-8.5	200,000
Harbour porpoise + Indo-Pacific bottlenose dolphin	105,000	3.9-8.5	200,000
Finless porpoise + Bottlenose dolphin	105,000	3.9-8.5	200,000
Finless porpoise + Indo-Pacific bottlenose dolphin	105,000	3.9-8.5	200,000
Finless porpoise + Killer whale	105,000	3.9-8.5	200,000
Finless porpoise + Long-finned pilot whale	105,000	3.9-8.5	200,000
Finless porpoise + Pacific white-sided dolphin	105,000	3.9-8.5	200,000
Harbour porpoise + Killer whale	105,000	3.9-8.5	200,000

Harbour porpoise + Long-finned pilot whale	105,000	3.9-8.5	200,000
Harbour porpoise + Pacific white-sided dolphin	105,000	3.9-8.5	200,000
Harbour porpoise + Finless porpoise	40,000	0.3-1.4	100,000
Indo-Pacific Bottlenose dolphin + Bottlenose dolphin	20,000	0.2-1.2	100,000
Indo-Pacific bottlenose dolphin + Killer whale	50,000	0.9-2.1 & 3.4-7	200,000
Indo-Pacific bottlenose dolphin + Long-finned pilot whale	50,000	0.9-2.1 & 3.4-7	200,000
Indo-Pacific bottlenose dolphin + Pacific white-sided dolphin	50,000	0.9-2.1 & 3.4-7	200,000
Bottlenose dolphin + Killer whale	50,000	0.9-2.1 & 3.4-7	200,000
Bottlenose dolphin + Long-finned pilot whale	50,000	0.9-2.1 & 3.4-7	200,000
Bottlenose dolphin + Pacific white-sided dolphin	50,000	0.9-2.1 & 3.4-7	200,000
Long-finned pilot whale + Killer whale	60,000	0.9-2.1 & 3.4-7	200,000
Pacific white-sided dolphin + Killer whale	50,000	0.9-2.1 & 3.4-7	200,000
Pacific white-sided dolphin + Long-finned pilot whale	50,000	0.9-2.1 & 3.4-7	200,000

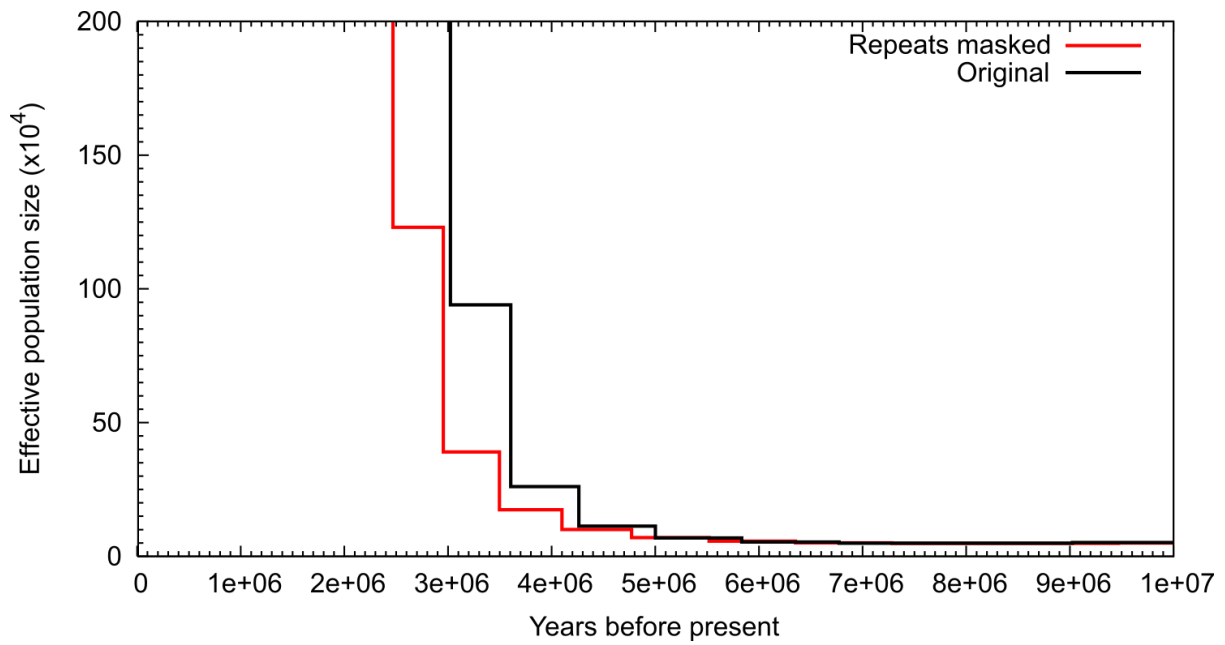
Supplementary figures



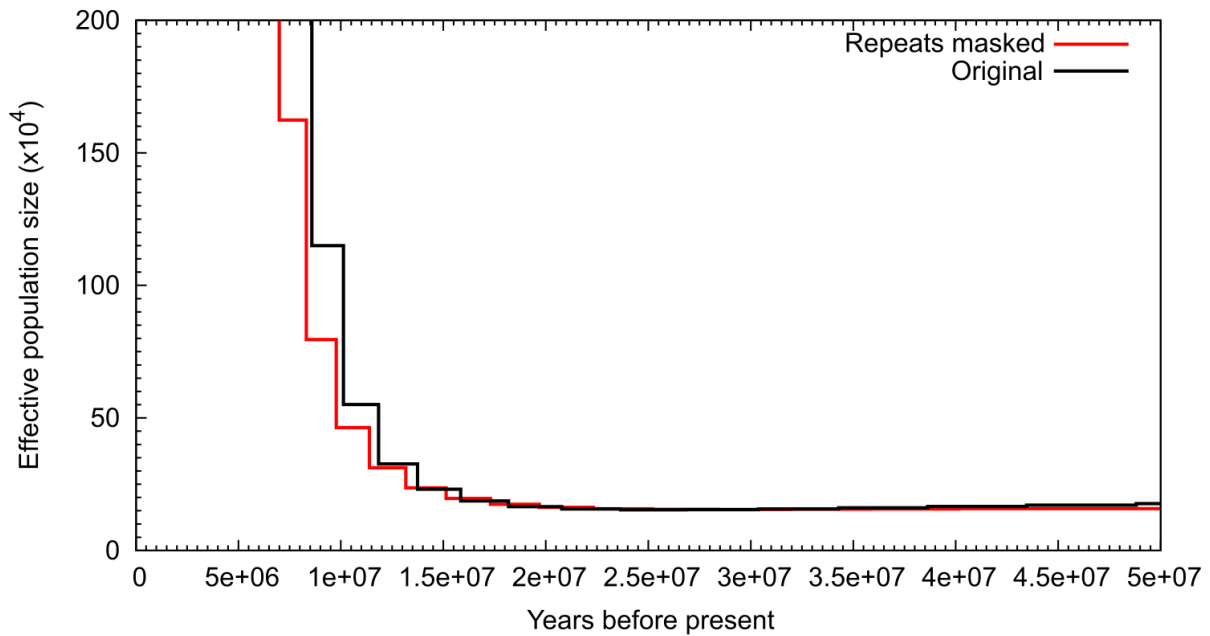
Supplementary figure S1: Consensus trees of independent Maximum-Likelihood trees constructed from non-overlapping sliding windows of (A) 1 Mb, (B) 500 kb, (C) 100 kb, or (D) 50 kb in length. Branch numbers represent the number of independent trees supporting each node.



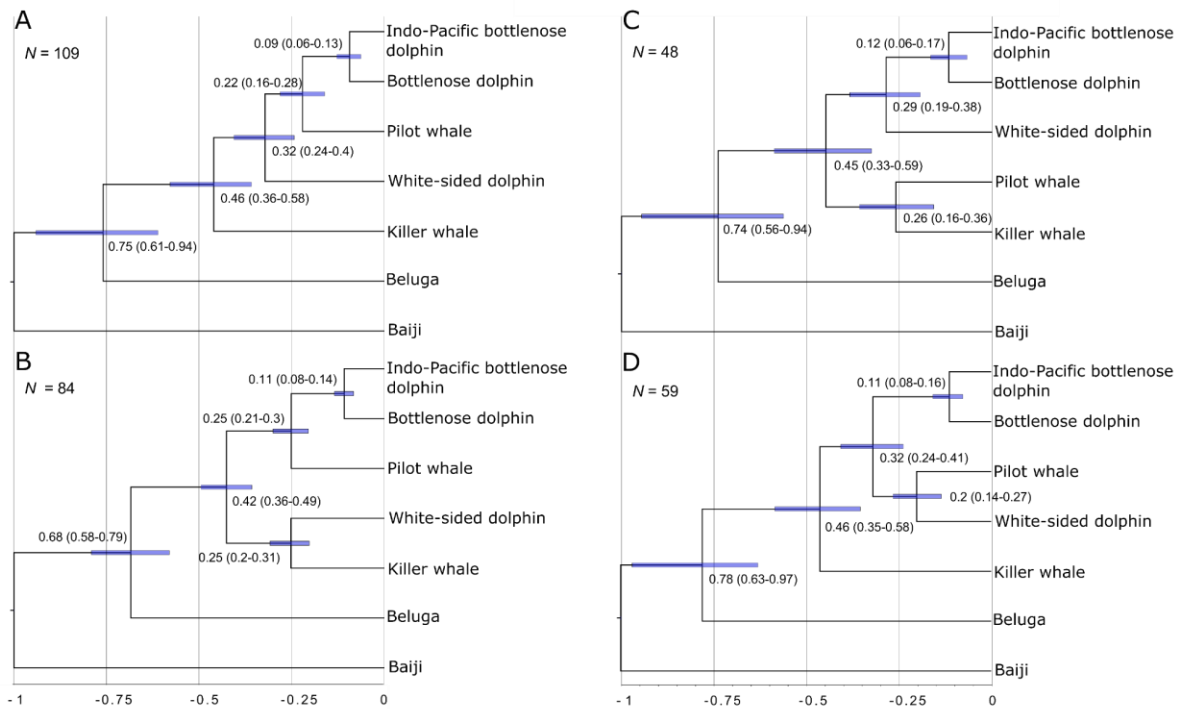
Supplementary figure S2: Comparison of hPSMC results using a pseudodiploid sequence from the bottlenose and Indo-Pacific bottlenose dolphins (shallow divergence) with either repeat regions masked or not.



Supplementary figure S3: Comparison of hPSMC results using a pseudodiploid sequence from the beluga and narwhal (medium divergence) with either repeat regions masked or not.



Supplementary figure S4: Comparison of hPSMC results using a pseudodiploid sequence from the bottlenose dolphin and beluga (deep divergence) with either repeat regions masked or not.



Supplementary figure S5: Relative divergence times of alternative topologies assumed to arise due to incomplete lineage sorting (ILS) or gene flow. N represents the number of independent loci supporting said topology. A) Consensus species topology. B) ILS/gene flow between the killer whale and Pacific white-sided dolphin. C) ILS/gene flow between killer whale and long-finned pilot whale. D) ILS/gene flow between Pacific white-sided dolphin and the long-finned pilot whale. Blue bars and numbers in parentheses show 95% credibility intervals.

Supplementary results

Additional plots of the hPSMC empirical and simulated data can be found under the following link: https://sid.erda.dk/cgi-sid/lis.py?share_id=ewvczfS2hH on the University of Copenhagen's electronic research data archive (ERDA). Bold lines show the hPSMC empirical data, faded lines show the simulated data, and the black lines show the simulated data that most closely match the empirical data without overlapping it between 1.5x and 10x the pre-divergence N_e .

Supplementary references

- Birkun AA Jr, Frantzis A. 2008. *Phocoena phocoena* ssp. *relicta*. The IUCN Red List of Threatened Species : e.T17027A50369903. <https://dx.doi.org/10.2305/IUCN.UK.2020-2.RLTS.T17027A50369903.en>.
- Footo AD, Vijay N, Ávila-Arcos MC, Baird RW, Durban JW, Fumagalli M, Gibbs RA, Hanson MB, Korneliussen TS, Martin MD, Robertson KM, Sousa VC, Vieira FG, Vinař T, Wade P, Worley KC, Excoffier L, Morin PA, Gilbert MTP, Wolf JBW. 2016. Genome-culture coevolution promotes rapid divergence of killer whale ecotypes. *Nat Commun* **7**:11693.
- Garde E, Hansen SH, Ditlevsen S, Tvermosegaard KB, Hansen J, Harding KC, Heide-Jørgensen MP. 2015. Life history parameters of narwhals (*Monodon monoceros*) from Greenland. *J Mammal* **96**:866–879.
- McGowen MR, Tsagkogeorga G, Álvarez-Carretero S, Dos Reis M, Struebig M, Deaville R, Jepson PD, Jarman S, Polanowski A, Morin PA, Rossiter SJ. 2020. Phylogenomic Resolution of the Cetacean Tree of Life Using Target Sequence Capture. *Syst Biol* **69**:479–501.
- Taylor BL, Chivers SJ, Larese J, Perrin WF. 2007. Generation length and percent mature estimates for IUCN assessments of cetaceans (No. Administrative Report LJ-07-01). National Marine Fisheries Service, Southwest Fisheries Science Center.
- Zhou X, Guang X, Sun D, Xu S, Li M, Seim I, Jie W, Yang L, Zhu Q, Xu J, Gao Q, Kaya A, Dou Q, Chen B, Ren W, Li S, Zhou K, Gladyshev VN, Nielsen R, Fang X, Yang G. 2018. Population genomics of finless porpoises reveal an incipient cetacean species adapted to freshwater. *Nat Commun* **9**:1276.

Triplet analysed	Geneflow pair	outgroup	Proportion of windows with gene flow	BIC2Dist (IBS + Geneflow)	BIC1Dist (IBS alone)	BIC difference	Significant for gene flow (BIC difference <10)	Number of trees	Percentage of total trees (2161) from triplet	Percentage of trees supporting topology explained by gene flow
Indo-Pacific Bottlenose dolphin_Bottlenose dolphin_K	Bot-Orca	Indo-Pacific Bottlenose	1	-47.1718	-40.833	-6.34	No	4	0.19	1.09
Pilot whale_Bottlenose dolphin_Killer whale	Bot-Orca	Pilot whale	0.994524	-4176.75	-4015.52	-161.23	Yes	363	16.80	44.13
White-sided dolphin_Bottlenose dolphin_Killer whale	Bot-Orca	White-sided dolphin	0.932662	-5203	-5001.75	-201.25	Yes	451	20.87	51.55
Indo-Pacific Bottlenose dolphin_Bottlenose dolphin_K	Indo-Orca	Bottlenose dolphin	1	-35.0559	-32.055	-3.00	No	3	0.14	0.37
Pilot whale_Indo-Pacific Bottlenose dolphin_Killer whale	Indo-Orca	Pilot whale	0.994149	-4163.39	-4003.35	-160.04	Yes	362	16.75	44.27
White-sided dolphin_Indo-Pacific Bottlenose dolphin_K	Indo-Orca	White-sided dolphin	0.936622	-5157.77	-4961.79	-195.98	Yes	448	20.73	91.82
Pilot whale_Indo-Pacific Bottlenose dolphin_Bottlenose dolphin	Pilot-Bot	Indo-Pacific Bottlenose	1	-56.1656	-53.3674	-2.80	No	5	0.23	1.09
Pilot whale_Indo-Pacific Bottlenose dolphin_Bottlenose dolphin	Pilot-Indo	Bottlenose dolphin	0.26425	-43.6088	-44.5198	0.91	No	4	0.19	0.15
Pilot whale_Bottlenose dolphin_Killer whale	Pilot-Orca	Bottlenose dolphin	0.89395	-4149.09	-3995.26	-153.83	Yes	353	16.34	26.63
Pilot whale_Indo-Pacific Bottlenose dolphin_Killer whale	Pilot-Orca	Indo-Pacific Bottlenose	0.894701	-4145.01	-3991.4	-153.61	Yes	353	16.34	24.46
White-sided dolphin_Pilot whale_Killer whale	Pilot-Orca	White-sided dolphin	0.890091	-5551.99	-5354.47	-197.52	Yes	479	22.17	30.52
White-sided dolphin_Pilot whale_Bottlenose dolphin	Pilot-White	Bottlenose dolphin	0.885824	-5329.17	-5126.07	-203.10	Yes	459	21.24	44.05
White-sided dolphin_Pilot whale_Indo-Pacific Bottlenose dolphin	Pilot-White	Indo-Pacific Bottlenose	0.883297	-5332.08	-5127.41	-204.67	Yes	459	21.24	37.09
White-sided dolphin_Indo-Pacific Bottlenose dolphin_Killer whale	White-Bot	Indo-Pacific Bottlenose	0.99938	-53.2849	-53.8868	0.60	No	5	0.23	0.46
White-sided dolphin_Pilot whale_Bottlenose dolphin	White-Bot	Pilot whale	0.870174	-7160.67	-6929.73	-230.94	Yes	629	29.11	86.33
White-sided dolphin_Indo-Pacific Bottlenose dolphin_Killer whale	White-Indo	Bottlenose dolphin	0.859332	-41.6525	-42.3186	0.67	No	4	0.19	0.31
White-sided dolphin_Pilot whale_Indo-Pacific Bottlenose dolphin	White-Indo	Pilot whale	0.871914	-7154.12	-6919.18	-234.94	Yes	628	29.06	49.33
White-sided dolphin_Bottlenose dolphin_Killer whale	White-Orca	Bottlenose dolphin	0.974941	-5679.95	-5365.25	-314.70	Yes	478	22.12	29.40
White-sided dolphin_Indo-Pacific Bottlenose dolphin_Killer whale	White-Orca	Indo-Pacific Bottlenose	0.975064	-5687.27	-5373.09	-314.18	Yes	479	22.17	31.43
White-sided dolphin_Pilot whale_Killer whale	White-Orca	Pilot whale	0.953523	-6205.88	-5910.93	-294.95	Yes	529	24.48	50.04

Triplet analysed	Geneflow pair	outgroup	Proportion of windows with gene flow	BIC2Dist (IBS + Geneflow)	BIC1Dist (IBS alone)	BIC difference	Significant for gene flow (BIC difference <10)	Number of trees	Percentage of total trees (2730) from triplet	Percentage of trees supporting topology explained by gene flow
Indo-Pacific Bottlenose dolphin_Bottlenose dolphin_Killer whale	Bot-Orca	Indo-Pacific Bottl	0.82	-143.55	-144.83	1.28	No	13	0.48	0.39
Pilot whale_Bottlenose dolphin_Killer whale	Bot-Orca	Pilot whale	0.64	-5877.09	-5828.01	-49.08	Yes	543	19.89	12.79
White-sided dolphin_Bottlenose dolphin_Killer whale	Bot-Orca	White-sided dolp	0.68	-6493.50	-6410.93	-82.57	Yes	589	21.58	14.76
Indo-Pacific Bottlenose dolphin_Bottlenose dolphin_Killer whale	Indo-Orca	Bottlenose dolph	0.85	-82.72	-81.61	-1.11	No	8	0.29	0.25
Pilot whale_Indo-Pacific Bottlenose dolphin_Killer whale	Indo-Orca	Pilot whale	0.67	-5836.61	-5777.56	-59.05	Yes	539	19.74	13.24
White-sided dolphin_Indo-Pacific Bottlenose dolphin_Killer whale	Indo-Orca	White-sided dolp	0.69	-6501.26	-6417.36	-83.90	Yes	590	21.61	14.82
Pilot whale_Indo-Pacific Bottlenose dolphin_Bottlenose dolphin	Pilot-Bot	Indo-Pacific Bottl	0.80	-306.79	-305.15	-1.64	No	28	1.03	0.82
Pilot whale_Indo-Pacific Bottlenose dolphin_Bottlenose dolphin	Pilot-Indo	Bottlenose dolph	0.46	-330.52	-336.87	6.35	No	31	1.14	0.52
Pilot whale_Bottlenose dolphin_Killer whale	Pilot-Orca	Bottlenose dolph	0.48	-5643.28	-5648.29	5.01	No	521	19.08	9.13
Pilot whale_Indo-Pacific Bottlenose dolphin_Killer whale	Pilot-Orca	Indo-Pacific Bottl	0.51	-5701.86	-5699.31	-2.55	No	525	19.23	9.77
Pilot whale_White-sided dolphin_Killer whale	Pilot-Orca	White-sided dolp	0.55	-6892.35	-6861.90	-30.45	Yes	631	23.11	12.75
Pilot whale_White-sided dolphin_Bottlenose dolphin	Pilot-White	Bottlenose dolph	0.59	-7033.39	-6989.18	-44.21	Yes	648	23.74	14.00
Pilot whale_White-sided dolphin_Indo-Pacific Bottlenose dolphin	Pilot-White	Indo-Pacific Bottl	0.59	-7073.33	-7026.60	-46.73	Yes	651	23.85	14.15
Pilot whale_White-sided dolphin_Bottlenose dolphin	White-Bot	Pilot whale	0.51	-9197.44	-9186.93	-10.51	Yes	865	31.68	16.05
White-sided dolphin_Indo-Pacific Bottlenose dolphin_Bottlenose d	White-Bot	Indo-Pacific Bottl	0.63	-257.04	-258.27	1.24	No	24	0.88	0.56
Pilot whale_White-sided dolphin_Indo-Pacific Bottlenose dolphin	White-Indo	Pilot whale	0.49	-9117.94	-9115.68	-2.26	No	858	31.43	15.41
White-sided dolphin_Indo-Pacific Bottlenose dolphin_Bottlenose d	White-Indo	Bottlenose dolph	0.40	-170.67	-176.49	5.81	No	16	0.59	0.23
Pilot whale_White-sided dolphin_Killer whale	White-Orca	Pilot whale	0.67	-8498.20	-8408.06	-90.14	Yes	784	28.72	19.25
White-sided dolphin_Bottlenose dolphin_Killer whale	White-Orca	Bottlenose dolph	0.75	-7986.93	-7853.23	-133.70	Yes	726	26.59	19.83
White-sided dolphin_Indo-Pacific Bottlenose dolphin_Killer whale	White-Orca	Indo-Pacific Bottl	0.75	-7983.67	-7846.07	-137.60	Yes	726	26.59	20.03

